SKYLAB EXPERIMENT S-019
ULTRAVIOLET STELLAR ASTRONOMY

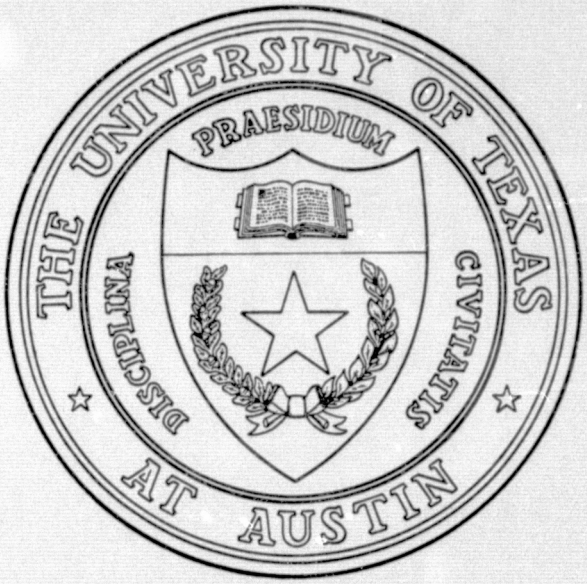

ONE YEAR REPORT

Submitted in accordance with Contract NAS 9–13176

Karl G. Henize, Principal Investigator
Department of Astronomy
University of Texas at Austin
Austin, Texas 78712

December 1975

SKYLAB EXPERIMENT S-019
ULTRAVIOLET STELLAR ASTRONOMY

ONE YEAR REPORT

Submitted in accordance with Contract NAS 9–13176

Karl G. Henize, Principal Investigator
Department of Astronomy
University of Texas at Austin
Austin, Texas 78712

December 1975

Distribution

Goddard Space Flight Center

M. Dubin, Code 680.0
T. Kelsall, Code 601
A. Underhill, Code 670

Johnson Space Center

P. Armitage, Code TA
Y. Kondo, Code TN23
S. Mansur, Code TN
R. Parker, Code CB

Marshall Space Flight Center

C. Lundquist, Code ES01
J. Williams, Code ES31

NASA Headquarters

T. Calio, Code SD
N. Hinners, Code S
N. Roman, Code SG
J. Rosendhal, Code SG
A. Schardt, Code SG

University of Texas

G. Benedict
K. Henize
S. Parsons
H. Smith
J. Wray

F. O'Callaghan - Boller & Chivens Division, Perkin-Elmer Corp., S. Pasadena, CA

G. Courtes - Laboratorie d'Astronomie Spatiale, Marseilles France

Experiment S-019
Personnel

Principal Investigator

Dr. Karl Henize	Johnson Space Center University of Texas, Austin

Deputy Principal Investigator

Dr. James D. Wray	University of Texas, Austin

Scientific Staff

Dr. Sidney B. Parsons	University of Texas, Austin
Dr. George F. Benedict	University of Texas, Austin

Affiliated Co-Investigators

Dr. Yoji Kondo	Johnson Space Center
Mr. Fred O'Callaghan	Boller & Chivens Division Perkin-Elmer Corporation

CONTENTS

ONE YEAR REPORT - SKYLAB EXPERIMENT S019

I. HISTORY AND BACKGROUND

A. History - This project originated at Dearborn Observatory, Northwestern University, in Evanston, Illinois. In 1965, Dr. Henize, having undertaken a survey of stellar spectra in middle UV wavelengths (2400-4000A) from Gemini spacecraft, proposed a more comprehensive survey reaching fainter stars and shorter wavelengths with a 15-cm aperture UV telescope mounted on the scientific airlock in the hatch of the Apollo command module. The proposal was accepted and the design and construction of the telescope was contracted to Cooke Electric Co. of Morton Grove, Illinois.

The design included a novel modification of the Ritchey-Chretien telescope configuration employing LiF and CaF_2 field correctors near the focal plane to provide sharp image quality over a 4° x 5° field at wavelengths extending from 1300 to 5000 A. Another novel feature was the use of a 15-cm diameter prism of CaF_2 to disperse the light. Although the availability of CaF_2 crystals of this size had been advertised it was soon discovered that the UV transmission of such large crystals was less than might be desired. This technical obstacle was finally overcome by a cooperative program in which the vacuum testing facility at Northwestern University was utilized to measure the transmission curves of numerous experimental crystals grown by Harshaw Chemical Co. until, at last, a suitable crystal was obtained.

Unfortunately the Apollo fire in early 1967 resulted in the removal of the scientific airlock from the hatch of the command module. Since the construction and most of the testing of the S019 telescope had been completed it was proposed to incorporate it into the Apollo Applications Program which later came to be named the Skylab Program. Operation of the telescope from Skylab required three major additions to or modifications of the equipment: (1) a quick-change mechanism was provided so that film canisters could be easily installed on and removed from the optical canister, (2) an articulated mirror system was required to allow the telescope line of sight to reach a large area of sky without need for maneuvering Skylab itself and (3) a spectrum widening mechanism was required to widen the spectra so that

fine spectral detail could be distinguished from photographic grain noise (in the Apollo concept the widening was to be accomplished by motion of the command module). The basic designs for these modifications were devised by F. G. O'Callaghan at Northwestern University and a prototype of the articulated mirror system was constructed in the Lindheimer Astronomical Research Center shops. The construction of flight hardware and its testing was contracted to the Boller and Chivens Division of Perkin-Elmer Corporation.

The construction and testing of flight equipment was completed in late 1972. At this time, the Principal Investigator (PI) transferred his academic affiliation to the University of Texas at Austin and the remainder of the project was carried out there. Key personnel who contributed to the Northwestern University phase of the program included: Dr. James D. Wray, Deputy Principal Investigator (after Dr. Henize became a scientist-astronaut in 1967), Mr. Fred G. O'Callaghan, Chief Engineer, and Mr. Lloyd Wackerling, Staff Astronomer.

A new staff was formed at the University of Texas under Dr. Wray who transferred from Northwestern University. This group was responsible for planning the observing program, support of the operational aspects of each mission and for data reduction and analysis. In addition to Dr. Wray, this group included Dr. Sidney B. Parsons, Dr. George F. Benedict and Dr. Paul M. Rybski.

The experiment was operated on each of the three Skylab missions and a total of 424 exposures were made on 219 star fields. The total number of spectra obtained was somewhat greater than pre-mission expectations. The volume of data and the complexity of measuring and correcting it to the desired accuracy are such that data analysis is only partially complete at the time of this report.

B. Background

The primary purpose of Experiment S019 was to obtain moderate dispersion stellar spectra in the wavelength region from 1300 to 3000 A with sufficient spectral resolution to permit the study of ultraviolet (UV) line spectra and of the spectral energy distribution of early-type stars. The data were expected to be of sufficient resolution and photometric accuracy to permit detailed physical analysis of

individual stars and nebulae, but an even more basic consideration was the expectation of obtaining spectra of a sufficient number of stars so that a statistically meaningful survey might be made of the UV spectra of a wide variety of star types. These should include nearly all spectral and luminosity classes of normal O, B and A stars as well as statistically meaningful numbers of peculiar stars such as Wolf-Rayet stars, Be stars and Ap stars.

The spectral resolution achieved (2 A at 1400 A) is about five times greater than that achieved by the first Orbiting Astronomical Observatory (OAO-A2) and is roughly equivalent to that generally achieved by sounding rocket spectrographs. The resolution is much less than that achieved by OAO-C but considerably fainter stars can be reached with the S019 equipment and the 1400 - 2000 A wavelength region is a region in which OAO-C performance is affected by serious noise problems. Thus, the S019 data are unique and serve in many ways as a bridge between the low resolution OAO-A2 data and the very high resolution data of OAO-C.

Although the S019 data are competitive with the sounding rocket spectra it is noteworthy that up to the time Skylab was launched, spectra of only about 30 stars had been obtained by sounding rockets whereas the Skylab instrument obtained spectra of 400 stars giving useful information at 1500 A. A sample of the spectra obtained and the spectral features visible in them is given in Figure 1. (See also Figure 2 of Appendix A and Figure 4 of Appendix F.)

II. INSTRUMENTATION

The instrumentation consisted of three basic components: the optical system, the film magazine (or canister) and the articulated mirror system (AMS). Taken together, the optical system and the film magazine are referred to as the spectrograph. Figure 3 in Appendix F shows a photograph of the assembled instrument with the articulated mirror extended. An explanatory diagram of this equipment is given in Figure 1 of Appendix A.

Since a detailed description of the instrument is given in Appendix

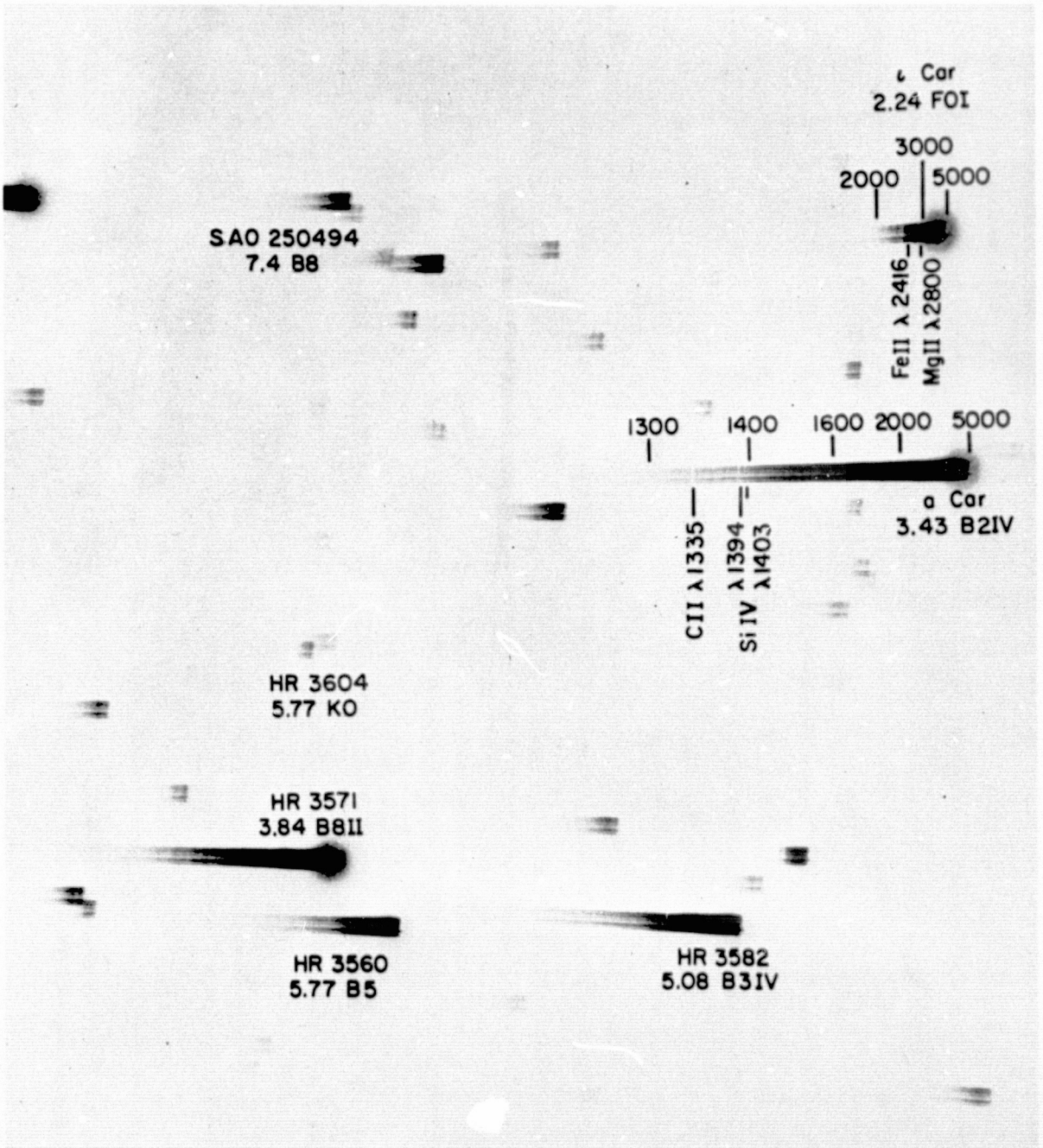

Figure 1. S019 Spectra in the Region of a Carinae. A wavelength scale is indicated above the spectra of a and ι Carinae and line identifications are noted below these spectra. Spectral classifications and V (visual) magnitudes are given for each identified star.

F, only a brief summary will be given here. The spectrograph optical system consists of a 15-cm aperture f/3 Ritchey-Chretien telescope with an achromatized two-element (CaF_2 and LiF) focal plane corrector, achieving 15 arcsec (34 μm) image diameters over a flat 4° x 5° field. Dispersion is provided by a 4° objective prism of CaF_2 which gives dispersions of 58, 350 and 1300 A mm^{-1} at 1400, 2000 and 2800 A, respectively. The resolutions achieved at these wavelengths in better-quality spectra are 2, 12 and 42 A.

Interchangeable film canisters each contained 160 frames of Kodak 101 film mounted on individual stainless steel backing plates. Ten frames in each canister were reserved for preflight and postflight calibration.

The articulated mirror system was used to allow pointing the telescope line of sight at various parts of the sky while Skylab maintained solar inertial pointing. The mirror system, with telescope attached, was mounted on the antisolar scientific airlock permitting the 38- by 19-cm flat mirror to be extended outside the spacecraft. Rotation and tilt controls allowed access to a band of sky 30° wide and 360° in circumference. Widening of the spectra was accomplished by a mechanism that slowly tilted the rear of the mirror canister through an angle of 270 arcsec, thus producing a spectrum width of 0.6 mm. This motion could be accomplished in either 270, 90 or 30 s. The slowest widening rate, one arcsec s^{-1}, made possible the recording of useful flux data at 1500 A for nominally reddened B0 stars with V = 6.5

The spectrograph could also be operated without spectral widening, in which case the effective exposure was set by the rate of spacecraft drift. Drift rates as small as 0.1 arcsec s^{-1} were frequently achieved, giving data on stars 2-3 mag fainter than the limit for widened spectra. Unwidened spectra were obtained in a total of 60 fields.

The operation of the instrument was entirely manual. The astronaut-observers pointed the mirror, verified (during the first operation of each mission) the mirror pointing by observing stars in the finding telescope, advanced film, opened and closed the shutter and timed exposures.

III. FLIGHT OPERATIONS

A. Observation Planning. Basic planning for S019 observations involved: (1) study of the Bright Star Catalogue (plus catalogues of peculiar hot stars such as Wolf-Rayet stars) to locate those fields rich in bright stars of classes O and B which were particularly suited to objective-prism spectroscopy and (2) devising computer programs and graphical displays to decide what fields were observable at a given time and to compute AMS tilt and rotation angles.

The selection of stars fields was begun at Northwestern University by Mr. Lloyd Wackerling and final refinements were made after the move to the University of Texas, primarily by Dr. Sidney Parsons. A total list of about 200 fields was eventually submitted to NASA for incorporation into their computer data banks. However, provisions were made to enter new fields at any time, and this option was used several times during the three missions.

Devising computer programs to calculate the position of any star field relative to the earth's horizon (i.e. altitude and azimuth) and relative to the AMS rotation axis (i.e. tilt and rotation angles) was a routine task. Two graphical aids to observational planning bear special mention, however. The first was a rectangular plot of the sky on which were plotted all star fields, the region of the sky at which the AMS can be pointed, the position of the earth's horizon at the times of sunset, midnight, and sunrise, and the moon's position. Such plots, produced for each operation period of S019, provided an easy means of selecting those fields visible at any particular time during the operation and were generally used for this purpose. They also provided a rough graphical means for verifying the calculated tilt and rotation angles since the position of the field within the observable band could be translated to tilt and rotation with little difficulty. One of these plots is illustrated in Figure 2.

The plotting program was first devised at Northwestern University. It was then used at the University of Texas to provide detailed advanced planning as well as final selection of star fields for the individual

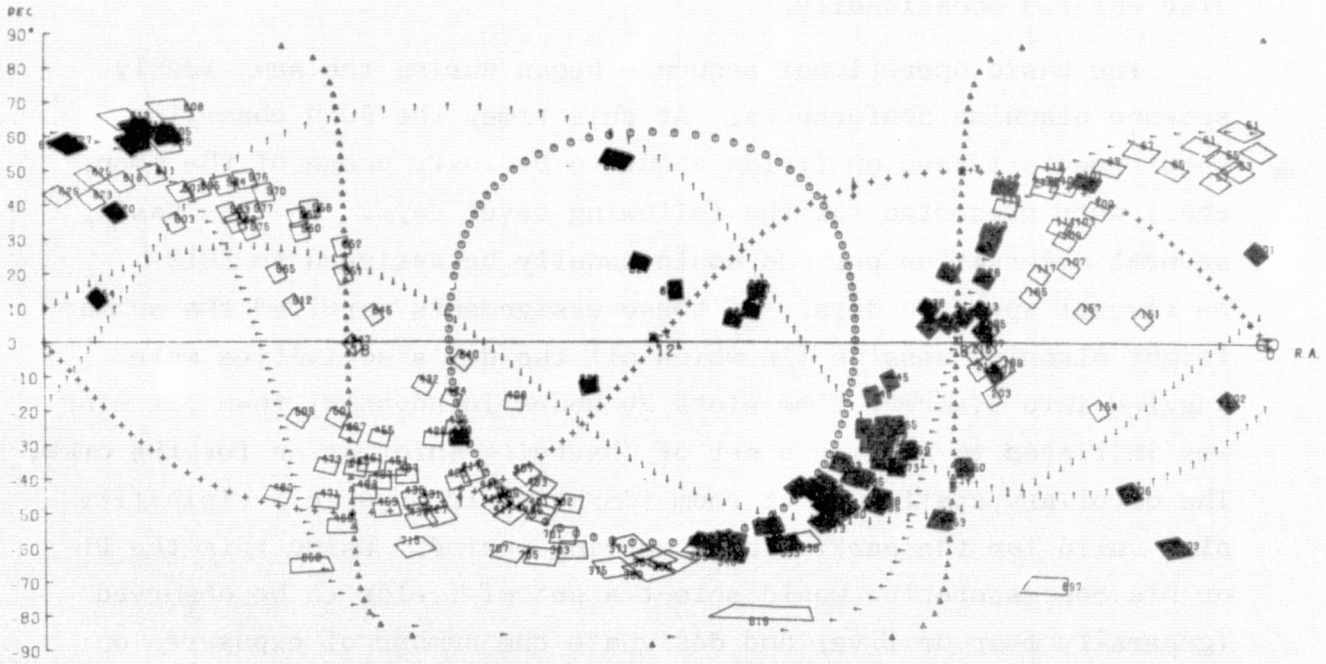

Figure 2. Sky Distribution of All Fields Photographed by Skylab Experiment S019. Fields photographed during Skylab 4 are shown in black. The fields are superposed on an operations planning plot for 23 March. The zone between the circles and the triangles is the region observable with the AMS on that date. Crosses show the projection of the orbit plane on the sky. The arrows, ↓ , ← and ↑ , indicate the earth's horizon at sunset, midnight and sunrise respectively.

observational periods. The plot was incorporated into the JSC planning system with minor modifications (more frequent plots of the earth's horizon were included) and was thus made available to all users of the AMS system.

The second planning system was a chart showing the observability of each field on each day of the mission. This facilitated broad strategic planning, e.g., identification of fields about to pass out of the observable region, identification of dates when many fields or few fields would be visible, etc. These charts were also used to identify dates on which observation of a given field were particularly desirable. These dates were set mainly by particular field orientations

which eliminated obvious overlapping of bright stars, but other factors such as presence of planets, phase of variable stars, etc. also entered occasionally.

The basic operational sequence began during the semi-weekly science planning conferences. At this time, the S019 observing requirements (based on fields about to be lost, phase of the moon, etc.) were presented for the following seven days. On this basis, several observation periods would usually be assigned to S019 on several specific days. If these assignments survived the summary flight planning session (in which all the day's activities were juggled into discrete time slots 24 hours in advance) then planning was initiated to provide a set of observing information for the crew. The corollary staff support room (CSSR) would produce a visibility plot valid for the particular observing period. Using this the PI or his representative would select a set of fields to be observed (generally four or five) and designate the number of exposures on each field and their times of beginning and ending. With this information the CSSR personnel would then calculate rotation and tilt angles and assemble them into a standard message format for transmission to the crew via teleprinter. An example of such a message and its explanation is given in Figure 3.

B. Mission Chronology

Date (UT)	Event
6, 8 March	SL2 film calibrated (canister 004)
10 March	SL2 film loaded (canister 004)
11 March	SL2 film canister 004 delivered to KSC
14 May	SL1 launched
15 May	Replacement SL2 film calibrated (canister 005)
17 May	Replacement SL2 film loaded (canister 005)
19 May	Replacement SL2 film canister 005 delivered to KSC
25 May	SL2 launched
30 May	First activation of AMS. Jamming of AMS tilt control discovered
31 May	Tilt control repaired by Paul Weitz

31 May	First activation of S019. Twelve exposures attempted but failed due to improper actuation of film advance lever
5 June	Operated for one orbit. First successful exposures
6 June	Operated for one orbit
17 June	Operated for two orbits with prism off
25 June	PI received film canister
25 June	SL3 film calibrated (canister 003)
27 June	SL3 film loaded (canister 003)
22, 28 June	SL3 film calibrated (canister 005)
29 June	Post-flight calibration of canister 005 film
4 July	Development of film from canister 005
9 July	SL3 film canister 003 delivered to KSC
11 July	SL3 film loaded (canister 005)
12 July	SL3 film canister 005 delivered to KSC
28 July	SL3 launched
4 August	Operated for one orbit
10 August	Operated for three orbits
13 August	Operated for one orbit
15 August	Operated for two orbits
16 August	Operated for two orbits
17 August	Operated for one orbit with prism off
20 August	Operated for two orbits, first with prism off
20 August	AMS refused to retract after second operation
21 August	AMS successfully retracted. Operated for one orbit
22 August	Operated for two orbits
23 August	Operated for two orbits
25 August	Operated for one orbit with prism off
28 August	Operated for three orbits, first with prism off
29 August	Operated for one orbit
30 August	Operated for three orbits
1 September	Operated for two orbits
3 September	Operated for one orbit
5 September	Operated for four orbits
7 September	Operated for one orbit

11 September Operated for one orbit

15 September Operated for two orbits

21 September Operated for two orbits. Film canister 005 jammed after exposure of one frame on first orbit. Film canister 003 used on second orbit

27 September PI received film canisters

2, 3 October Post-flight calibration of canister 003 film

4 October Replacement AMS mirror aluminized at GSFC

5 October Development of film from canister 003

9 October Post-flight calibration of canister 005 film

10 October Development of film from canister 005

18 October SL4 film calibrated (canister 003)

19 October SL4 film calibrated (canister 002)

26 October SL4 film loaded (canisters 002 and 003)

28 October SL4 film canisters 002 and 003 delivered to KSC. Replacement AMS mirror delivered to KSC

16 November SL4 launched

25 November Operated for one orbit

26 November Operated for one orbit

4, 5 December Operated for one orbit

7 December Operated for one orbit

8 December Operated for one orbit

12 December Operated for one orbit

13 December Operated for one orbit

14 December Operated for one orbit

16 December Operated for one orbit

17 December Operated for one orbit (Comet Kohoutek only)

19 December Operated for one orbit

20 December Operated for two orbits

24 December Operated for one orbit. Film canister 002 jammed after three exposures

30 December Operated for three orbits

2 January 1974 Failure of tens and hundreds digits of rotation counter of AMS

5 January Operated for two orbits

7, 8 January Operated for one orbit. Canister 003 jammed. Jam was freed by force

8 January	Operated for one orbit
12 January	Operated for one orbit (Comet Kohoutek only). Canister 003 jammed after one exposure. Attempt to free by force resulted in breaking drive shaft.
12 January	Attempt to free canister 002 by force apparently successful (but not in reality)
14 January	Operated for one orbit (Comet Kohoutek only). Shift on zero point of AMS rotation detected
25 January	Operated for two orbits
30, 31 January	Operated for one orbit
11 February	PI received film canisters
13, 14 February	Post-flight calibration of canister 003 film
15 February	Post-flight calibration of canister 002 film
21 February	Development of film from canister 002. Development of film from canister 003.

C. Equipment Malfunctions

1. Jamming of AMS tilt mechanism (SL2) - During the first activation of the AMS the mirror tilt mechanism was found to be jammed. Diagnosis based on crew comments and study of the training unit indicated that a sealing plate added at the last minute to the tilt counter was probably touching a gear with a very high mechanical advantage thus preventing rotation of the tilt knob. Repair procedures for removing the knob and the gear housing and for freeing the gear were transmitted to the crew. These were implemented by Paul Weitz who found the diagnosis to be correct. He corrected the problem and restored the AMS to normal operation.

2. Leak in film canister 005 (SL2) - When canister 005 was opened after the flight to remove the film it was found to have lost its vacuum. Testing revealed a leak in the reticule seal of the finder eyepiece which was easily repaired. At first it was suspected that this leak was responsible for the hole-pattern fog which appeared on the films. It was reasoned that contaminants from the spacecraft atmosphere had condensed on the metal plates and produced the fog. However, a similar fog appeared on film from all canisters subsequently flown and it was therefore concluded that the leak was in no way responsible for the hole-pattern fog.

```
3417              S019 PAD          34/242   01
------------------CDR-----------------        02
NUZ -4.1        CASS 003        PRISM  IN     03
STRT     ROT     TILT  FLD     EXPOSURES      04
1240    232.5    10.9  463     270/90/30      05
1247    249.8    06.6  467      270/270U      06
1257    031.2    13.5  065            270     07
1301    057.4    28.3  111            270     08
1306    049.6    21.0  100     270/90/30      09
                             SUNRISE  1312    10
REMARKS:  NO STABILIZATION                    11
VERIFICATION REQUIRED                         12
--------------------------------------        13
3417              S019 PAD              EOM   14
```

Figure 3. Typical S019 Observational Data Message.

Line 1 - gives message number (3417), experiment identification, mission day (34) and day of year 242 (30 Aug.)

Line 2 - states crew member (commander) to carry out the observation

Line 3 - gives NUZ - the assumed correction for spacecraft roll about the Z-axis (-4°.1), the film cassette to be used (003) and whether the prism is to be in or out

Line 4 - gives column headings

Line 5 - gives time to start exposure 1 (1240 UT), the rotation setting (232°.5), the tilt setting (10°.9), the field number (463), and exposure times (270 sec, 90 sec, and 30 sec)

Lines 6 - 9 - give similar data for exposures 2 through 5. The "U" in line 6 indicates that that exposure is to be unwidened

Line 10 - states that the sun will rise at 1312. Exposures must be completed and the film hatch must be closed by that time

Lines 11 and 12 - give a special message that the unwidened exposure may be taken without verifying the attitude drift rate of the spacecraft

Line 14 - repeats the message number, the experiment identification and indicates the end of the message (EOM)

3. Failure of AMS to retract (SL3) - On 20 August, the AMS refused to retract after an operation. The diagnosis was that ice had formed on the AMS extension screws and had frozen the mirror in the extended position. This diagnosis was supported by the fact that just before the operation period when the mirror froze, the mirror and its extension mechanism,while still cool from a previous operation period,had been exposed to spacecraft atmosphere when the optical canister was removed from the mirror canister to change the prism. This sequence of events made it very probable that moisture from the spacecraft atmosphere had condensed on the extension screws just prior to the mirror being extended again. The only evident solution was to wait for the ice to sublimate, then try to retract the mirror again. Approximately 24 hours after the malfunction occurred this was attempted and the mirror broke free. Thereafter care was taken to avoid the possibility of water condensing on the AMS mechanisms and no further difficulties were encountered.

4. Failures of the slide transport system - Film canisters jammed on three separate occasions - canister 005 on SL3 and canisters 002 and 003 on SL4. The film jam in canister 005 could not be remedied and approximately 28 frames of film were left unused as a consequence. It was found in the laboratory that a screw had backed out of position and interfered with the motion of the film carriage.

The jams in canisters 002 and 003 were due to the slide transport systems. The proper adjustment of these systems is a delicate matter requiring two "claws" to engage the outside edge of each new film slide and to pull it into the slide carriage, at the same time forcing the old slide into the stack of exposed slides. Abnormal friction caused by improper compression in either the fresh-slide stack or the exposed-slide stack, or by a roughness in one of the slides might cause a claw to slip in which case a slide jam could result. Every precaution was taken to adjust stack compression properly, to inspect each slide for smoothness, and to cycle each load of slides completely after loading to ensure that all adjustments were correct. However, for reasons which are not completely clear, both canisters on SL4 did jam.

The first to jam was canister 002 on 24 December after 55 slides had been used. It was put into storage and canister 003 was used for subsequent observations. On 7 January canister 003 jammed after 75 frames had been transported. Ground analysis indicated that the only hope of solving the problem was to apply force to the film advance lever in hopes of freeing the jam. An attempt to do so was successful and eight more exposures were obtained before a second jam occurred on 12 January. An attempt to free this jam by force was unsuccessful, resulting in a hard internal jam, loss of synchronism in the drive mechanism and free cycling of the film advance lever. An attempt to free up canister 002 was apparently successful and fifteen more exposures were made with this canister. However when the film was developed it was found that the film transport had not operated during these final fifteen exposures.

5. Loss of luminescent material in the AMS tilt and rotation counters. During the Critical Design Review Skylab crew members requested that the AMS digital displays be illuminated so that the equipment might be operated without a flashlight. Since S019 had no electrical connection to Skylab, and since it was considered undesirable to create such an interface, it was decided to use luminescent paint to cause the numbers to glow. The luminescent material chosen was promethium, a radioactive alpha particle emitter. Extensive testing had indicated that the paint adhered well to the dials but shortly before the launch of SL1 one numeral on the training unit, which had seen excessive use, became detached. This led to the last minute adding of sealing plates to the tilt and rotation counters to ensure that no radioactive material could migrate into the spacecraft atmosphere. Although this action was the cause of the initial jam in the tilt mechanism (see section IIIC1), it proved ultimately to be a wise decision inasmuch as the paint began to chip off the counters in the course of SL3 and continued to do so until approximately 50% of the numerals were lost by the end of SL4.

Beyond the threat of radioactive contamination (which was successfully averted), the main impact of this failure was to make exact setting of the counters more difficult for the crew and to require the use of flashlights for careful setting near the end of SL4.

6. Failure of the tens and hundreds digits in the AMS rotation display (SL4) - This failure was due to a breaking of the linkage between the units and tens dials within the counter. Since the units and tenths digits continued to operated properly, it was possible to overcome this failure by counting revolutions of the drive wheel to the nearest tenth of a revolution. This provided a setting accurate to ±3° and final setting could then be achieved by use of the units and tenths digits of the counter. This change in operating procedures required a revision of the uplinked data format and a slight slowing of the operational time line but, in general, gave results of the same accuracy as had been previously achieved. The solutions to this failure and to the following one provided an excellent example of man's ability to work around minor equipment failures.

7. Shifting of zero-point in the AMS rotation display (SL4) - Late in the SL4 mission the crewmen detected shifts in the rotation readings at which the discone antennae could be sighted. These sightings were used subsequent to the failure of the 10's and 100's digits of the rotation counter to confirm the rotational zero position at which the mirror could be retracted. After star sightings confirmed that a shift in zero-point had taken place, sightings of the antennae were used prior to each observation period to confirm the position of zero rotation. Although this procedure produced accurate results, the complication of crew procedures required by this and the above failures resulted in a loss in efficiency of about 30%.

D. Sources of Data Degradation

1. Film fog - Four types of film fog may be distinguished on S019 films: (a) fog resulting from bright moonlight or twilight illumination of the AMS mirror, (b) a hole-pattern fog on those regions of the film not protected by the nylon covers, (c) a weak, uniform fog in the regions protected by the nylon covers and (d) a random blotchiness in the hole-pattern fog.

a. Fogging by moonlight had been anticipated and during SL2 a flight planning constraint required that S019 be scheduled only

when the moon was less than half illuminated. However, this considerably reduced the frequency and ease of scheduling S019 and, when trial exposures made during SL2 with a bright moon showed no appreciable fog, this constraint was dropped.

During SL3 one operation scheduled when the moon was near full and only 13 degrees off the axis of the anti-solar airlock resulted in a complete fogging of all frames exposed. Another operation with the moon 19 degrees off the airlock axis resulted in the fogging of only one frame. These data suggested that when the moon was very near the axis of the airlock, moonlight directly entering the airlock aperture around the mirror was producing intolerable fog. Therefore no SL4 operations were scheduled when the moon was less than 16° off the airlock axis. Other data suggested that appreciable fogging resulted whenever the moon shone directly onto the surface of the AMS mirror and such circumstances were avoided whenever possible during SL4. These measures eliminated problems with moonlight fogging during SL4.

However there was no way to shield the AMS mirror from the bright twilight when Comet Kohoutek was being observed. As a result all exposures of Comet Kohoutek show discernible background fog and in two instances the fog is excessive. It is suspected that in these two instances the hatch of the film canister was not closed prior to sunrise.

b. The hole-pattern fog duplicates the pattern of holes in the perforated stainless steel plates on which the films were mounted. Since it occurs only in the area of the film not protected by the nylon snap-on retainers it must be concluded that the fog results in some way from the proximity of the film to the stainless steel plate of the slide directly above it. (The metal areas are fogged and the holes show little fog, thus the effect cannot be due to light passing through the holes.) It is known that Kodak 101 emulsion is fogged by exposure to bare aluminum but the physics of the process are not well understood. It was not known that stainless steel would produce such an effect but it seems likely that such an effect (although in a much smaller degree) is responsible for the observed fog on S019 films.

It was reasoned that vacuum stowage would enhance the transfer of electrons from the metal to the film (if that were indeed the physical process involved) and that stowage with gas in the canister might surpress the effect. A laboratory test gave evidence that this was indeed the case but by this time the SL4 film had already been delivered to KSC with the film stowed in vacuum. However, once operations began, spacecraft atmosphere was admitted to the canister prior to stowage of the canister. Although the evidence is somewhat inconclusive, the fact that the hole-pattern fog of SL4 does not greatly exceed that of SL3 suggests that the procedure may have had some helpful effect.

c. The weak uniform fog observed in regions protected by the nylon covers is presumably due to a combination of thermal fog and fog produced by radiation-belt particles. In Figure 4 the degree of such fog on film in each film canister flown is plotted against the total radiation dose calculated for each canister. The proportionality

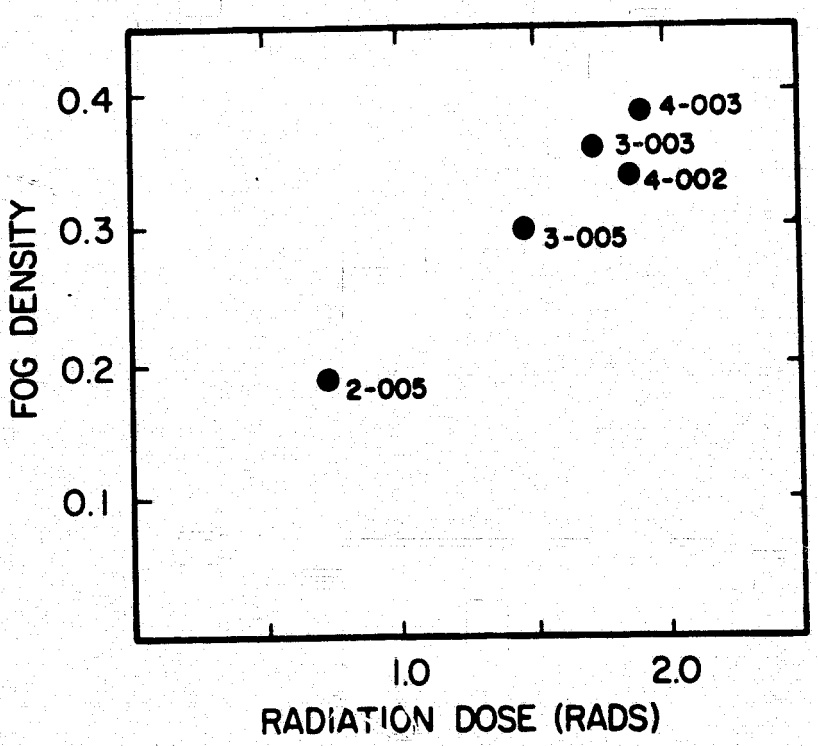

Figure 4. Density of Fog vs. Radiation Dose for S019 Film Canisters. This fog is measured in the regions protected by the nylon covers.

of fog to dose suggests that this fog is indeed due primarily to radiation-belt particles. However, there is also a proportionality (though with greater scatter) with mission duration (i.e., with exposure to adverse thermal environment) and it should be emphasized that these two effects cannot be clearly separated.

The effects of the radiation environment were anticipated and operating procedures were devised to minimize the time intervals during which the film canisters were outside the film vault. Both intervals inside and outside the film vault are properly accounted for in the doses indicated in Figure 4.

d. The blotchy background fog tended to have a characteristic dimension of 10 to 20 mm and frequently had a form resembling a fingerprint at the edge of the frame. It was suspected that this fog was due to contamination of the steel plates as they were handled during film loading. Precautions were taken to prevent this during all film loadings and extreme care in this respect was exercised during the loading of SL4 film. However, the extra care made no appreciable difference in the frequency of occurrence of these blotches.

It should be noted that research at the Naval Research Laboratory (NRL Report 7072) indicates that Kodak 101 film is prone to blotchy fogging (they note a characteristic dimension of 15x30mm) due to several environmental effects including vibration and long-term exposure at room temperature to either normal atmosphere or to gaseous nitrogen. Thus the blotches observed may be due to a number of factors.

2. AMS mirror reflectivity - After the condensation episode of 20, 21 August (condensation had been noted on the mirror surface during these operations) it was suspected that the UV reflectivity of the AMS mirror may have been affected and approval was given to provide a replacement mirror for SL4. A fresh UV-reflective coating for this mirror was kindly supplied on an emergency basis by Goddard Space Flight Center.

When the SL3 film was inspected, it was evident that the reflectivity at 1500 A had indeed decreased by a factor of 2 to 3 toward the end of the SL3 mission and final approval was given for the SL4 crew to carry the replacement mirror into orbit. They completed the mechanical

task of removing the old mirror and inserting the new one without undue difficulty.

Data derived from experiment S201 indicate that this new mirror suffered appreciable loss of reflectivity at 1200 A on about 12 December. An analysis of S019 data concerning changes in mirror reflectivity is not yet complete.

3. Pointing errors - Pointing errors of ±0.1 to ±0.2 degrees were generally experienced and had little effect on the quality of the data. However, larger errors were occasionally experienced and resulted in loss of data on a number of stars. The primary cause for this was inadequate knowledge of spacecraft attitude, especially roll about the Z axis. Although a star tracker was available to determine this aspect of attitude, recent data were not always avaliable and errors of ±1 degrees in pointing occasionally occurred.

A less frequent cause of pointing errors was mistakes by the crew. In two instances, an erroneous value for the mirror rotation was set and used and in two other instances the correction for rotation about the Z-axis was applied with the wrong sign.

4. Stabilization - At least 50% of the exposures obtained for S019 were affected by streakiness in the spectra and/or by non-orthogonality in their widening. The streakiness might be due either to spacecraft attitude jitter or to jumps in the motion of the widening mechanism. However, the fact that image excursions occur with about the same frequency in the direction of dispersion (producing non-orthogonal widening) as in the perpendicular direction (producing streaks) leads to the conclusion that the streakiness is mainly due to spacecraft attitude jitter. ATM measures of spacecraft stability under the impact of crew motions during SL3 confirm that normal crew motion created a continual jitter with excursions as large as ±60 arcsec frequently occurring. Since the image diameter produced by the S019 optics is 15 arcsec, excursions for several seconds with ranges from 10 to 60 arcsec are just the type required to produce the observed streaks.

In general, the crews had been requested to avoid violent motion and exercise when S019 was being operated, but use of the bicycle

ergometer (a smooth, cyclic motion) was not construed to be "violent motion". However, the ATM test indicated that significant excursions occurred when the ergometer was in use and this activity was also banned during S019 observations on SL4.

When the streaks were first observed subsequent to SL2 it was considered likely that they arose from vibrations of the airlock in the spacecraft wall due to the crewmen touching the equipment during exposures. However, even though this was carefully avoided during SL3 and SL4, little or no decrease in streakiness was observed. Nevertheless occasional loss of resolution at the beginning of an exposure is seen in the spectra, giving evidence that such flexures did produce vibrations when the spectrograph was affected by forces such as the actuation of the film advance lever.

Fortunately, the effect of streaks in the spectra and the non-orthogonal widening can be largely corrected by sophisticated data reduction techniques (see Section IV) and their main effect is the cost and inconvenience of this extra data processing.

5. Variability in the rate of spectrum widening - Although the spectrum widening mechanism was absolved from the production of the streaks in the spectra discussed above, it did have one unfortunate fault - its widening rates were 10 to 20% faster than expected (thus resulting in an 0.1 to 0.2 magnitude loss in limiting magnitude) and the rate was somewhat variable. When set for a 270 sec exposure the widening mechanism would complete its motion in anywhere from 210 to 270 sec. Since this interval was not predictable, the only method to obtain exact exposure times was via information given on the voice tapes. These are generally adequate although there are instances when the moment of exposure start or ending was not recorded or was lost in transmission.

IV. DATA REDUCTION

A summary of data reduction procedures is given in Section III of Appendix A. Only explanatory notes will be added here.

A. Rectification of irregularly widened spectra. A step-by-step explanation of this process is given in Figure 5. The end result of this processing may be either the tracing shown in step 3 or the processed photographic spectrum shown at the top.

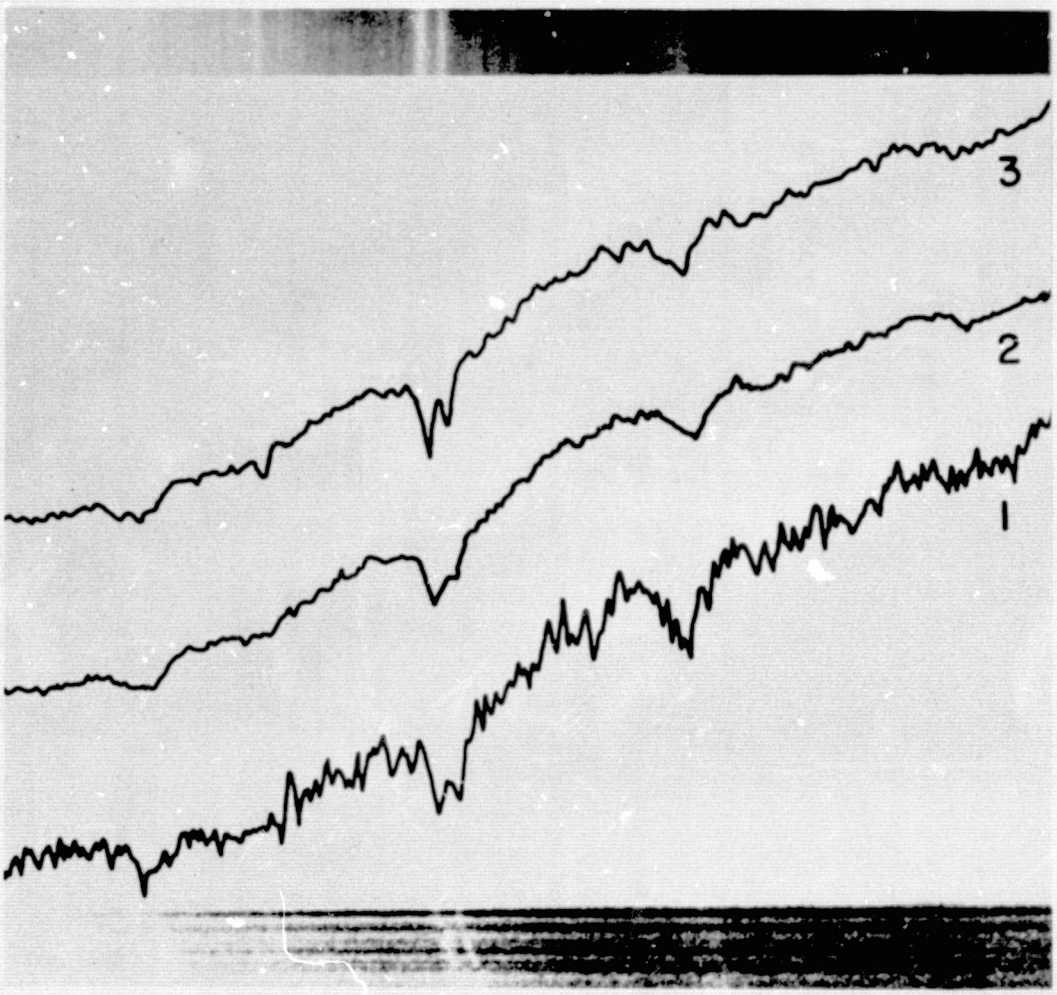

Figure 5. Rectification of Irregularly Widened Spectra.
Below. The original spectrum showing streaks and slanted lines.
1. Single scan with a 15 μm x 20 μm aperture.
2. Mean of 20 scans without wavelength shifts.
3. Mean of 20 scans after wavelength rectification.
Above. Photographic play-back of data shown in tracing 3. Several weak lines are now visible which were not clearly seen in the original spectrum.

B. D-Log I calibration. The graded exposures mentioned generally included 10 exposures at each wavelength at up to 13 separate wavelengths. These exposures were monitored by a sodium-salicylate coated photo cell so that the sensitivity function of the film and spectrograph could be determined in order that relative flux curves may be derived from these spectra. It is expected that these data may be confirmed by observations of several stars for which flux curves are already well known.

C. Wavelength scale. Due to the effects of lateral chromatic aberration and to optical distortion, the wavelength scale varies with position within the field. Knowledge of the empirical dispersion curve and its variation with position has evolved slowly as measures were made of more and more stars with easily identified spectral lines.

The dispersion curve is defined by:

$$\lambda = \frac{0.258}{x/f + 0.74 - \Delta} + 0.102$$

where λ is wavelength in microns, x is distance in mm measured from the long wavelength end of the spectrum, f is a stretch factor depending on field position and Δ is a small empirical correction depending on x/f. Values of Δ are given in Table 1. To facilitate computerized data reduction an analytic function has been fitted to empirical values of f. This function has the form:

$$f = a_0 + a_1 X + a_2 Y + a_3 XY^2 + a_4 X^2 + a_5 Y^2 + a_6 X\sqrt{|X|}$$

where
$a_0 = 0.9899$
$a_1 = -7.7882 \times 10^{-4}$
$a_2 = -9.3673 \times 10^{-6}$
$a_3 = +6.1586 \times 10^{-6}$
$a_4 = +2.4304 \times 10^{-4}$
$a_5 = +1.3290 \times 10^{-4}$
$a_6 = -3.6693 \times 10^{-4}$

X and Y are distances in mm measured from plate center on the original film. Positive values of X are in the direction of shorter wavelength.

Table 1

Tabulation of Wavelengths and Wavelength Correction Δ As a Function of Distance From Long Wavelength End of Spectrum

mm*	Δ	λ (Å)	Å/mm	mm*	Δ	λ (Å)	Å/mm
0.00	+.092	5000		4.20	.038	1546.3	
			7720				107
.10	.036	4228		.30	.036	1535.6	
			4230				103
.20	.014	3805		.40	.033	1525.2	
			2930				99
.30	+.005	3512		.50	.031	1515.3	
			2325				95
.40	-.002	3280		.60	.029	1505.8	
			1915				92
.50	-.008	3088		.70	.025	1496.5	
			1602				89
.60	-.012	2928		.80	.022	1487.6	
			1362				86
.70	-.016	2792		.90	.019	1479.0	
			1171				83
.80	-.019	2675		5.00	.016	1470.7	
			1017				80
.90	-.021	2573		.10	.013	1462.8	
			891				77
1.00	-.022	2484		.20	.010	1455.1	
			788				74
.10	-.023	2405		.30	.007	1447.6	
			700				72
.20	-.022	2335		.40	.004	1440.5	
			627				69.3
.30	-.020	2273		.50	+.001	1433.5	
			564				67.4
.40	-.017	2216		.60	-.003	1426.7	
			511				65.4
.50	-.013	2165		.70	-.007	1420.2	
			467				63.4
.60	-.009	2118		.80	-.010	1413.9	
			430				61.5
.70	-.005	2075		.90	-.014	1407.7	
			396				59.7
.80	.000	2036		6.00	-.017	1401.8	
			367				57.9
.90	+.005	1999		.10	-.021	1396.0	
			342				56.2
2.00	.010	1965		.20	-.025	1390.4	
			319				54.6
.10	.014	1933		.30	-.029	1385.0	
			298				53.0
.20	.019	1903		.40	-.033	1379.7	
			280				51.5
.30	.023	1875		.50	-.037	1374.5	
			262				50.0
.40	.028	1849		.60	-.041	1369.5	
			248				48.6
.50	.032	1824		.70	-.045	1364.7	
			236				47.3
.60	.035	1801		.80	-.049	1360.0	
			223				46.0
.70	.038	1778		.90	-.054	1355.3	
			210				44.8
.80	.041	1757		7.00	-.058	1350.9	
			201				43.7
.90	.043	1737		.10	-.063	1346.5	
			190				42.6
3.00	.045	1718		.20	-.068	1342.2	
			182				41.5
.10	.046	1700		.30	-.073	1338.0	
			173				40.5
.20	.047	1683		.40	-.077	1334.0	
			164				39.5
.30	.048	1666		.50	-.082	1330.0	
			156				38.6
.40	.049	1651		.60	-.087	1326.2	
			152				37.7
.50	.048	1635		.70	-.092	1322.4	
			143				36.8
.60	.048	1621		.80	-.097	1318.7	
			138				35.9
.70	.047	1607		.90	-.102	1315.1	
			132				35.0
.80	.046	1594		8.00	-.107	1311.6	
			127				34.2
.90	.044	1581		.10	-.113	1308.2	
			122				33.4
4.00	.042	1569		.20	-.118	1304.8	
			117				
.10	.040	1557.5					
			112				

*Distance must be measured in mm and divided by stretch factor f before entering the table.

D. Background subtraction. The subtraction of the hole pattern is an important consideration for those portions of the spectra with density less than one. Initially a sophisticated subtraction technique was devised in which the background in the region of the spectrum was estimated at 20 μm intervals by a curve fitting process which joined the sky background data on one side of the spectrum to that on the other side with a smooth curve. Empirical testing indicated this method produced results accurate to about ±2%. However, the complexity of the arithmetic was such that it could not be performed in the PDP-8/e computer which operated on-line with the microdensitometer. It was necessary to transfer the data to the University of Texas CDC 64/6600 computer. This was a time consuming process and made any sort of interactive judgment almost impossible. Therefore a simple linear interpolation from one side of the spectrum to the other which can be performed in the PDP-8/e has been adopted for most spectra. The estimated errors of background subtraction by this process are on the order of ±4%.

E. Mirror reflectivity. Changes in mirror reflectivity with date in the missions must be accounted for when stellar flux curves are studied. Preliminary data indicate that loss of reflectivity shortward of 1700A is much more severe than in the longward region. A number of star fields were photographed repeatedly so that such degradation might be measured. However, a final derivation of the reflectivity changes has been postponed until other factors affecting flux calibration have been more completely determined.

F. Vignetting. Geometrical studies indicate about a 30% loss of flux at the edge of the field compared to the center. It is expected that the vignetting function will be determined empirically by study of spectra in several overlapping fields taken for this purpose.

V. SCIENTIFIC RESULTS

During all three Skylab missions prism-on observations were obtained in 188 starfields and prism-off observations in 31 starfields. The distribution of the prism-on fields is shown in Figure 2. In general the fields are concentrated in the Milky Way where the frequency of hot stars is highest. These fields cover an area approximately

3660 degrees and include roughly 24 percent of a band 30° wide centered on the plane of the Milky Way.

A census of stars in the prism-on fields shows that nearly 6000 stars have measurable flux data at a wavelength of 2600A, that 1600 have measurable data at 2000A and that 400 show useful data at 1500A. Obvious absorption or emission features shortward of 2000A are visible in approximately 120 stars.

This represents a veritable bonanza of data useful for statistical studies of stellar classification and of interstellar reddening as well as for studies of various types of peculiar stars. Since the Copernicus telescope of OAO-C functions very poorly in the 1400-2000A region and since other survey instruments in this wavelength range (e.g. experiment S2/68 of the TD1 satellite) give much lower resolutions, the S019 data are unique and so far unduplicated in the 1400 to 2000A range.

Reprints or preprints of the first five technical papers based on these data are given in Appendices A through E to illustrate the various fields of astrophysics to which these data contribute. Appendix A shows how the strong lines of CIV and SiIV in the UV may be used to provide more sensitive temperature and luminosity classification criteria for O and early B stars than are available in visible wavelengths. The change in the CIV/SiIV intensity ratio in the temperature range from B1 to B0 is particularly dramatic. This change is illustrated in Figure 6 which also shows visible spectra of about the same resolution for these two spectral types. The visible spectra show only subtle changes in the weaker lines.

Also noteworthy in Figure 3 of Appendix A are the changes with luminosity of the SiIV lines at class O9 and the changes with luminosity of the CIV line at class B1. These are the most striking luminosity effects seen anywhere in the spectrum at any spectral type.

Another important result of this first quick survey of the spectra is the discovery that the emission-absorption profiles in the CIV and SiIV lines previously known to be characteristic of O and early B

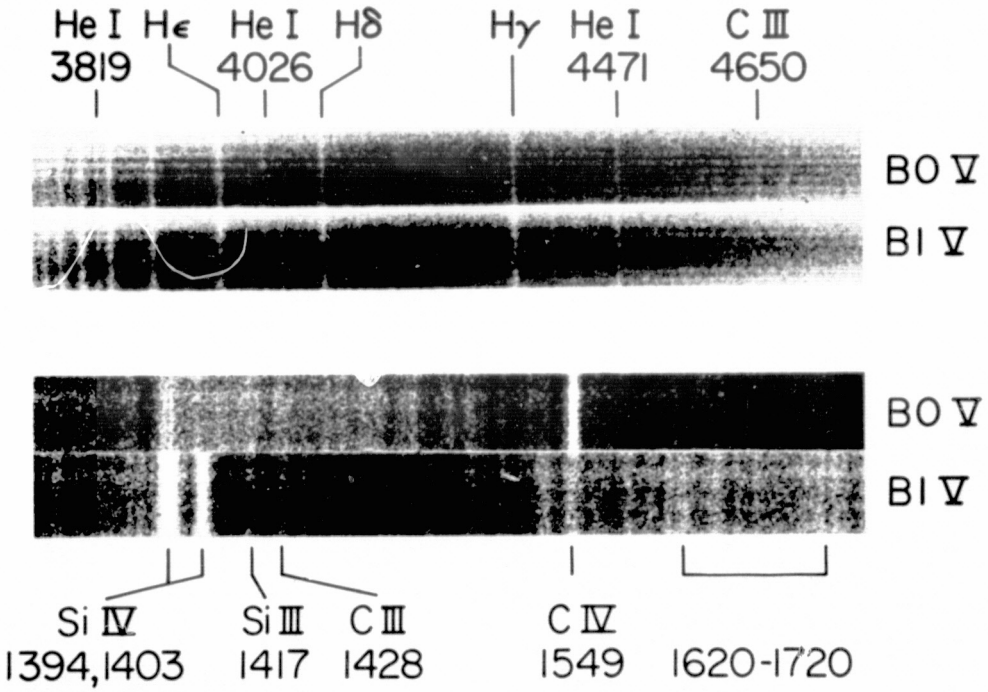

Figure 6. A Comparison of the Dramatic Changes in UV Line Strengths Between Spectral Types B0 and B1 with the Very Subtle Changes Seen in Visible Wavelengths.

supergiant spectra, are found also in lower luminosity classes in the hottest stars. This leads to the conclusion that all stars brighter than absolute bolometric magnitude -8.4 show this line profile which is indicative of largescale mass outflow from these stars.

Examples of how studies of peculiar stars have been advanced are given in Appendices B, C and D. In Appendix B data are presented on the UV emission lines of 12 Wolf-Rayet stars. Most Wolf-Rayet stars are quite faint and the OAO instruments have been able to produce data for only 3 Wolf-Rayet stars. Probably the most important

aspect of this paper is the discovery that in those stars with known hot supergiant companion stars, the spectrum of the companion is more dominant in the UV than in visible wavelengths. This has lead (1) to new conclusions on the temperatures of the Wolf-Rayet stars and (2) to the discovery of new companion stars from the UV observations.

Appendix C illustrates how UV spectral characteristics may conflict with spectral classification based on visible radiation. In the particular case of these rapidly rotating stars it is demonstrated that the UV spectral data will yield significantly more reliable stellar temperatures than will the visible light data. It is also possible that further investigation of those stars which show the most marked discrepancies will reveal new, previously unsuspected, physical characteristics in these particular stars.

Appendix D discusses a number of newly observed emission lines in the peculiar star β Lyrae. By astrophysical coincidence it appears that the predominant lines in the 1300 to 2300 A region arise from regions in this very complex system which are not easily observed at other wavelengths and that these data may provide interesting new insight into the outer halo of the β Lyrae system.

Appendix E illustrates the leverage available in these spectra for finding new examples of binary stars with hot but faint (at visible wavelengths) secondary components. HR3080 is the most outstanding example discovered in a quick visual survey of the spectra. It is expected that other such binaries will be found when fully calibrated flux data become available from the S019 spectra. These flux data will also allow determination of the temperature of the hotter components in known binary systems of this type.

The star HR6164 in Figure 2 of Appendix A and most of the Wolf-Rayet stars shown in Appendix B show a sudden cut off at 2200A which is due to the interstellar reddening peak which extends from 2000 to 2400 A. Nearly all hot stars show this feature in some degree and it is anticipated that the S019 data will allow statistical studies of this feature in stars fainter and more distant than has been possible up to now. The physical origin of this peak is not yet known and

questions concerning its correlation with other interstellar absorption features and concerning its variation in intensity from point to point in the Milky Way are highly controversial.

Another interesting aspect of the 2200A absorption feature is that, due to its great strength, it is expected that it may be used to estimate color excesses and total absorptions for peculiar stars whose intrinsic colors are difficult to determine because of their peculiarity. Such stars include the Wolf-Rayet stars, P Cygni stars, etc.

It is to be emphasized that the results to date involve mostly qualitative, classification-type data analysis and that fully calibrated flux data have not been available. The data reduction procedures to achieve fully calibrated fluxes are only just now becoming available. The availability of such data for large numbers of stars and the capability of comparing them with predicted data on a star-by-star basis will make possible many quantitative astrophysical studies.

Appendix A

SKYLAB ULTRAVIOLET STELLAR SPECTRA: VARIATION OF INTENSITY AND STRUCTURE OF STRONG LINES WITH TEMPERATURE AND LUMINOSITY

The Astrophysical Journal, Vol. 199, No. 2, Part 2, 1975 July 15

THE ASTROPHYSICAL JOURNAL, 199:L119–L121, 1975 JULY 15

SKYLAB ULTRAVIOLET STELLAR SPECTRA: VARIATION OF INTENSITY AND STRUCTURE OF STRONG LINES WITH TEMPERATURE AND LUMINOSITY

K. G. HENIZE, J. D. WRAY, S. B. PARSONS, G. F. BENEDICT, F. C. BRUHWEILER, AND P. M. RYBSKI
Department of Astronomy, University of Texas at Austin
AND
F. G. O'CALLAGHAN
Boller and Chivens Division, Perkin-Elmer Corporation
Received 1975 February 14; revised 1975 April 4

ABSTRACT

Objective-prism spectra at ultraviolet wavelengths extending to 1300 Å were photographed during the three *Skylab* missions in a survey covering 9 percent of the sky. Several spectral features, notably resonance lines of C IV and Si IV, show striking variations with stellar temperature and luminosity. Marked P Cygni profiles in C IV and Si IV, indicative of significant outflow of mass, appear in the spectra of all stars with M_{bol} brighter than -8.4.

Subject headings: early-type stars — spectra, ultraviolet

I. INTRODUCTION

This is the first report of data obtained with a 15-cm aperture objective-prism telescope (Experiment S-019) operated onboard the *Skylab* space station to obtain ultraviolet stellar spectra in the wavelength range from 1300 to 5000 Å. A total of 359 usable prism exposures in 188 star fields were made in the course of the three *Skylab* missions. These cover an area of approximately 3660 square degrees and include roughly 24 percent of a band 30° wide centered on the Gould belt.

A census of stars appearing in these fields shows that nearly 6000 stars have measurable flux data at wavelengths of 2600 Å or less. Of these, roughly 1600 have measurable data at 2000 Å or less, and 400 show useful data at 1500 Å or less. Obvious absorption or emission features shortward of 2500 Å are visible in approximately 170 stars.

II. INSTRUMENTATION

The telescope used to obtain these spectra is a 15-cm aperture f/3 Ritchey-Chrétien telescope with an achromatized two-element (CaF_2 and LiF) focal plane corrector, achieving 15″ (34 μ) image diameters over a flat 4° × 5° field. Dispersion is provided by a 4° objective prism of CaF_2, which gives dispersions of 64, 365, and 1281 Å mm^{-1} at 1400, 2000, and 2800 Å, respectively. The resolutions achieved at these wavelengths in better-quality spectra are 2, 12, and 42 Å.

Interchangeable film canisters each contained 160 frames of Kodak 101 film mounted on individual stainless steel backing plates. Ten frames in each canister were reserved for preflight and postflight calibration.

An articulated mirror system (see Fig. 1) was used to allow pointing the telescope line of sight at various parts of the sky while *Skylab* maintained solar inertial pointing. The mirror system, with telescope attached, was mounted on the antisolar scientific airlock permitting the 38- by 19-cm flat mirror to be extended outside the spacecraft. Rotation and tilt controls allowed access to a band of sky 30° wide and 360° in circumference. Widening of the spectra was accomplished by a mechanism that slowly tilted the rear of the mirror canister through an angle of 270″, thus producing a spectrum width of 0.6 mm. This motion could be accomplished in either 270, 90, or 30 s. The slowest widening rate 1″ s^{-1} made possible the recording of useful flux data at 1500 Å for nominally reddened B0 stars with $V = 6.5$.

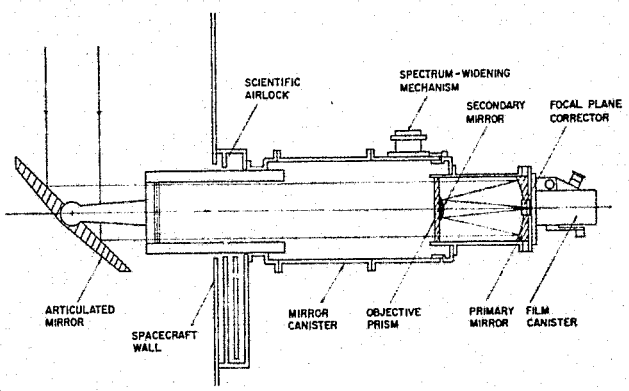

FIG. 1.—Schematic diagram of the S-019 spectrograph and the articulated mirror system mounted on the scientific airlock.

The spectrograph could also be operated without spectral widening, in which case the effective exposure was set by the rate of spacecraft drift. Drift rates as small as 0″.1 s^{-1} were frequently achieved, giving data on stars 2–3 mag fainter than the limit for widened spectra. Unwidened spectra were obtained in a total of 60 fields.

The operation of the instrument was entirely manual. The astronaut-observers pointed the mirror, verified (during the first exposures of each mission) the mirror

pointing by observing stars in the finding telescope, advanced film, opened and closed the shutter, and timed exposures.

A sample of spectra photographed with this equipment is illustrated in Figure 2 (Plate L6).

III. DATA REDUCTION PROCEDURE

The objective-prism spectra recorded with this instrument possess several properties which must be carefully accounted for in reducing the data. The most significant, in terms of their effect on data reduction procedures, are the effect of spacecraft motion on spectral widening, and the presence of a moderate film fog showing a hole pattern

Two types of spacecraft motion are frequently observed in these spectra: (*a*) slow drifts producing curved or slanted lines and (*b*) frequent small random jumps with amplitudes on the order of 50–100 μ in the focal plane. The random jumps may be either along or perpendicular to the dispersion axis, and their basic effect is to produce streaky spectra with irregular lines. Quantitative analysis of such spectra requires that each spectrum be scanned with a two-dimensional raster. Then conversion of density to intensity on a point by point basis in both x and y removes the ambiguities inherent in the quantitative analysis of streaky spectra. Shifting the scans parallel to the wavelength axis by an appropriate amount allows correction for the effects of curved or irregular lines, thereby maintaining the spectral resolution quoted in § II above.

For calibration, graded exposures at several wavelengths were made on flight film before and after flight and on laboratory film which was not flown. In this way the effect of the flight environment on the film could be deduced and accounted for. Preliminary (D, log I) data, based on sensitometric exposures on laboratory film, processed together with the flight film, have been used to reconstruct computer processed images of the spectra which are the principal subjects of this paper.

The (D, log I) calibration data are treated as a three-dimensional surface, the third coordinate being wavelength. This surface is entered into the computer as a two-dimensional array accessed by values of measured density and wavelength. In the spectra presented in this paper, wavelength is assigned on the basis of the system dispersion function referenced to some identifiable spectral line.

The hole pattern in the background fog appears to be due to exposure of the film to the perforated stainless steel backing plates. However, it is not clear whether the effect is due to the metal itself (Kodak 101 is known to fog rapidly when exposed to untreated aluminum) or to contaminants carried by or attracted by the metal. The average fog density in the regions between holes is roughly proportional to the time of exposure to the metal, reaching a value of 0.60 during the 100-day exposure of *Skylab 4*. Areas of the film covered by a nylon retaining frame do not show a hole pattern and exhibit an average fog density of 0.39 during the *Skylab 4* mission. This lighter fog is assumed to be a combination of thermal and radiation fog. The estimated radiation dose during *Skylab 4* that contributed to this effect was 1.91 rads.

Subtraction of the background hole pattern is accomplished by measuring background regions on both sides of the spectrum. The probable background in the region occupied by the spectrum is interpolated at each wavelength increment by a spline fit to the smoothed background data. The effect of background fog on the image of a calibrated step-wedge was found to behave linearly with effective exposure rather than with density, indicating that densities should be converted to intensities before the interpolation and subtraction are accomplished, a procedure we have adopted.

When two or more exposures are available on the same star, the individual spectra are combined in a weighted mean. The weight of each point in a spectrum depends primarily on its photographic density, those densities lying on the linear portion of the (D, log I) curve receiving the highest weights. In addition, since noise is greatest where the weights are lowest, a smoothing is introduced which is inversely proportional to the total weight at each point.

The reduction of the data is carried out primarily with a PDS 1010Å microdensitometer controlled by a PDP-8/e computer (Wray and Benedict 1974). Correction for background fog is accomplished with the CDC 64/6600 computer of the University of Texas. Finally an arbitrary adjustment is made to the mean slope of the continuum to allow the data to be displayed photographically for visual inspection over the entire wavelength range of the observed spectrum. Thus the appearance of the continuum is not indicative of the continuous energy distribution. Quantitative spectral energy distributions will be presented in subsequent papers.

IV. ULTRAVIOLET SPECTRA OF NORMAL STARS

Sixteen stars with normal spectra in the visible region are displayed in Figure 3 (Plate L7). Spectral types of stars earlier than B0 are those of Walborn (1972), while spectral types for B0 and later are on the revised MK system, from Morgan and Keenan (1973), Hiltner, Garrison and Schild (1969), or Lesh (1968). The major line features have been identified with the help of published rocket spectra by Morton *et al.* (1972).

Four very prominent lines appear in this wavelength region: C IV λ1549, Si IV λλ1394, 1403, and C II λ1335. The striking variations in the absorption strengths of these lines may be summarized as follows. The C IV absorption strengthens rapidly with temperature between B2 and B0 and then remains more or less constant in the earlier spectral types. At spectral class B1 the C IV strength shows an unusually strong correlation with luminosity, increasing from nearly zero in class V stars to very strong in supergiants. In O stars the correlation is still evident but the total change in strength is less extreme.

In luminosity class V stars, Si IV absorption peaks sharply at spectral class B1 and has virtually disappeared at class O9.5. In luminosity class I stars, on the

other hand, Si IV remains strong in the O stars. This effect is unexpected since if the weakening of Si IV in main-sequence stars hotter than B1 is due to the ionization to Si V, then at temperatures equal to or greater than those of B1 dwarf stars the Si IV strength should decrease with increasing luminosity rather than increase. This phenomenon is added evidence for extended atmospheres with extreme departures from local thermodynamic equilibrium in O and early B supergiant stars.

The ratio of Si IV to C IV in luminosity class V and III stars shows a dramatic reversal between classes B1 and B0 and makes possible very fine discrimination of spectral classes in this range. This reversal is not so apparent in the supergiant stars because of effects mentioned above. In class V stars the λ1335 line of C II shows remarkably little variation in strength from A0 through O9.5 but appears to reach a peak in intensity in the B2-B5 range. Between B1 and B3 the C II/Si IV ratio is an excellent temperature criterion. Although the C II/Si IV ratios illustrated in Figure 3 are felt to be representative, there are several instances in our spectra where this ratio deviates from the norm for a given spectral class. These stars will be a subject of future investigation.

Emission on the longward side of the C IV and Si IV resonance lines together with increased width of the absorption appears to be a widespread phenomenon in the hottest and most luminous stars. Figures 3*c* and 3*d* clearly illustrate that when emission becomes evident, the C IV and Si IV absorptions show a large shift to shorter wavelengths whereas the weaker absorption lines and blends do not. This P Cygni phenomenon has been noted before in rocket spectra of O9 and B0 supergiants (Morton 1967), but now a large enough sample of stars is available for more comprehensive studies. A borderline for its definite occurrence runs diagonally across the H-R diagram, from O7 V to O9.5 III to B3 Ia. This result is consistent with the ground-based studies of Hutchings (1970) and Rosendhal (1973), which pointed toward a limiting bolometric luminosity above which significant mass outflow occurs. With the new bolometric corrections and effective temperatures of Code *et al.* (1975), the $T_{\rm eff}$ scale of Conti (1974), other work scaled to these, and absolute magnitudes from Walborn (1973) and Lesh (1968), we place this mass loss border at $M_{\rm bol} \approx -8.4$.

A number of the weaker features show positive luminosity effects. The region from 1640 to 1720 Å is discussed by Jenkins, Morton, and York (1974) over a limited spectral range (B0–2 III–V) in which they find sensitive temperature criteria, but no strong luminosity indicators except perhaps a blend near 1720 Å. We find that the absorption blends in the 1620–1720 Å region are enhanced in some supergiants near B0, especially in μ Nor. This strengthening is not apparent in all supergiants in the O9–B1 range and may be an indication of extreme luminosity. The 1720 Å feature, which includes N IV and Al II, was first discussed by Underhill, Leckrone, and West (1972) on the basis of OAO-2 scans, which showed the feature strong in supergiants from A2 to B0. We confirm this result and find that the feature also is present in O stars, with maximum strength near O8 I.

The concept for this experiment was originated at Northwestern University by Henize, where he, O'Callaghan, and Wray were responsible for the design and development of the spectrograph, constructed by Cook Electric Co., and of the articulated mirror system, constructed by Boller & Chivens Division, Perkin-Elmer Corp. We are grateful to the many individuals in NASA, especially the three *Skylab* crews, whose dedicated efforts contributed immeasurably to the success of the experiment. We thank Dr. A. Strobel, Mrs. Y. Strobel, and Mrs. L. Krizan for their help with the census of stars, and Messrs. B. Cuthbertson and D. West for their assistance in data reduction. We also wish to acknowledge the help of Mr. L. Wackerling of Northwestern University who contributed to the formulation of the observing program. This project is currently supported at the University of Texas under NASA contract NAS 9-13176.

REFERENCES

Code, A. D., Davis, J., Bless, R. C., and Hanbury Brown, R. 1975, submitted to *Ap. J.*
Conti, P. S. 1974, *Ap. J.*, **179**, 181.
Hiltner, W. A., Garrison, R. F., and Schild, R. E. 1969, *Ap. J.*, **157**, 313.
Hutchings, J. B. 1970, *M.N.R.A.S.*, **147**, 161.
Jenkins, E. B., Morton, D. C., and York, D. G. 1974, *Ap. J.*, **194**, 77.
Lesh, J. R. 1968, *Ap. J. Suppl.*, **17**, 371.
Morgan, W. W., and Keenan, P. C. 1973, *Ann. Rev. Astr. and Ap.*, **11**, 29.
Morton, D. C. 1967, *Ap. J.*, **147**, 1017.
Morton, D. C., Jenkins, E. B., Matilsky, T. A., and York, D. G. 1972, *Ap. J.*, **177**, 219.
Rosendhal, J. D. 1973, *Ap. J.*, **186**, 909.
Underhill, A. B., Leckrone, D. S., and West, D. K. 1972, *Ap. J.*, **171**, 63.
Walborn, N. R. 1972, *A.J.*, **77**, 312.
———. 1973, *A.J.*, **78**, 1067.
Wray, J. D., and Benedict, G. F. 1974, *Proc. Soc. Photo-Opt. Instr. Engineers*, **44**, 137.

G. F. Benedict, F. C. Bruhweiler, S. B. Parsons, P. M. Rybski, and J. D. Wray: Department of Astronomy, University of Texas, Austin, TX 78712

K. G. Henize: NASA/Johnson Space Center, Code TE, Houston, TX 77058

F. G. O'Callahan: Boller & Chivens, Perkin-Elmer Corp., 916 Meridian Avenue, South Pasadena, CA 91030

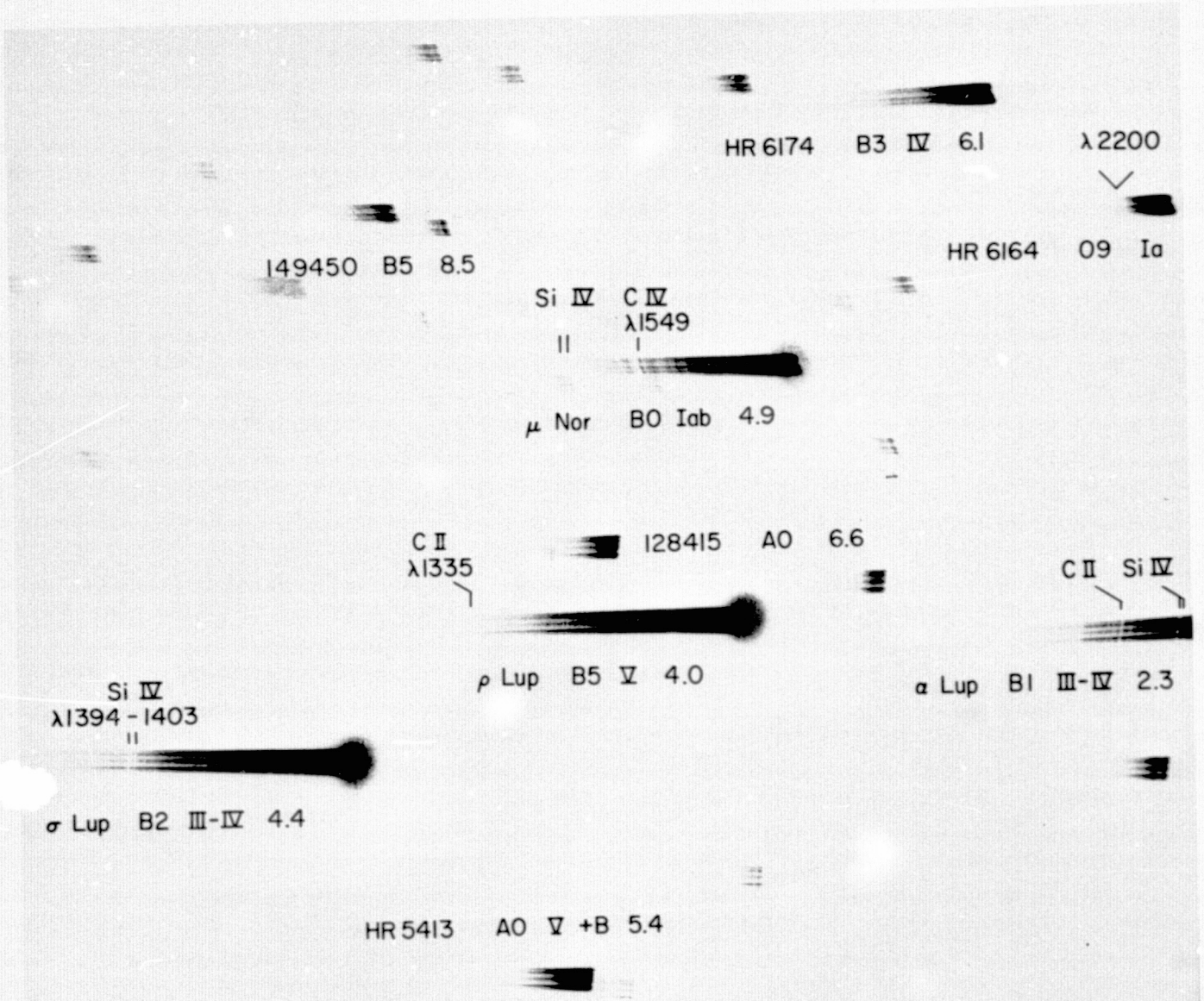

FIG. 2.—Portions of two fields of objective-prism ultraviolet spectra. Identifications, spectral types, and visual magnitudes are indicated for several stars. P Cygni profiles in C IV and Si IV are evident in μ Nor. The effect of the interstellar absorption peak at 2200 Å is seen in the heavily reddened ($E[B - V] \approx 0.7$) O9 Ia star HR 6164. The absorption "line" seen near the long-wavelength end of several faint stars is the Balmer discontinuity.

HENIZE *et al.* (*See* page L120)

PLATE L7

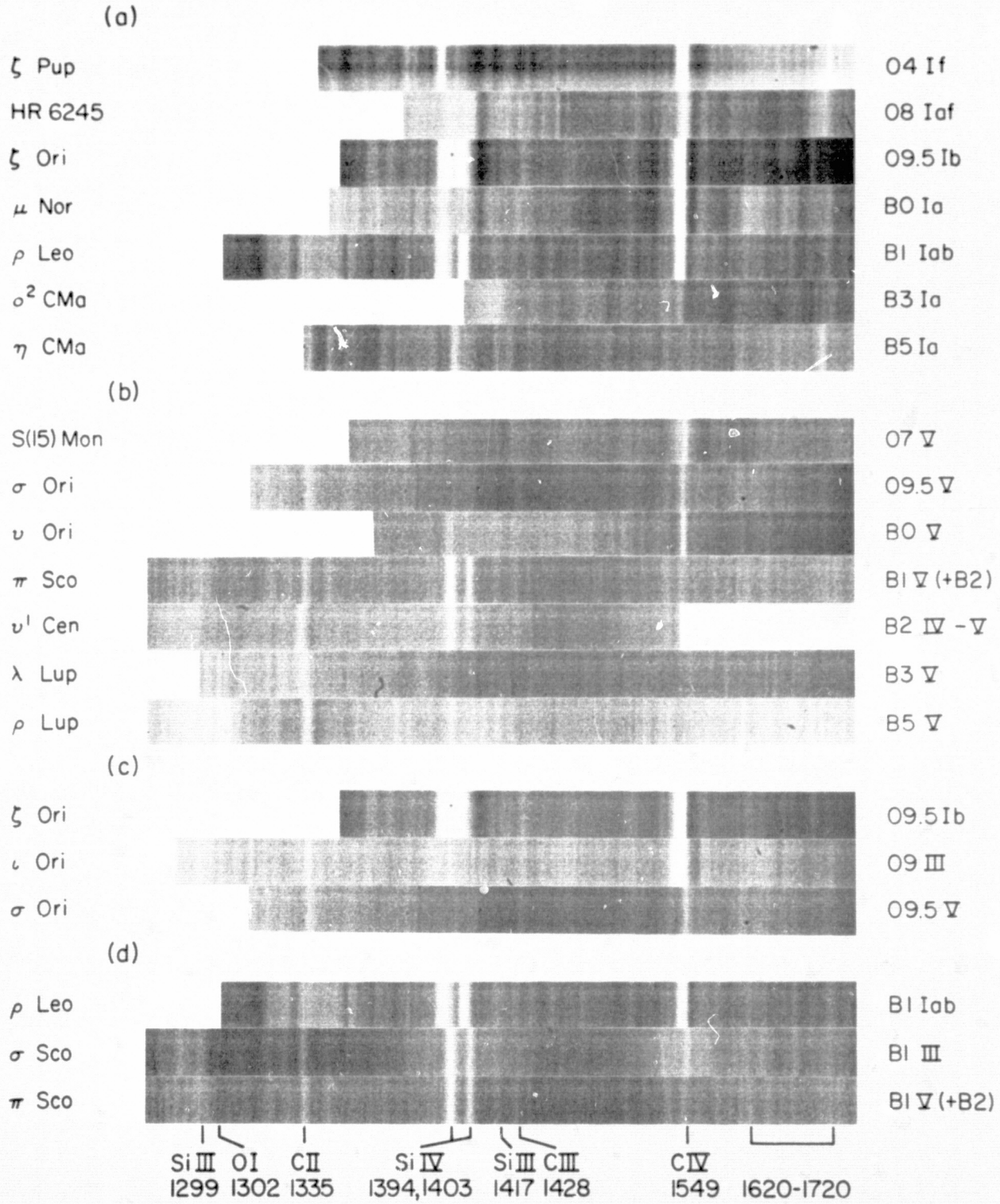

FIG. 3.—Rectified spectra of representative stellar types in the region 1300–1800 Å. (*a*) Temperature effects among supergiants, (*b*) temperature effects along the main sequence, (*c*) luminosity effects at O9–O9.5, (*d*) luminosity effects at B1. Two or three spectra of each star are averaged (see text). Although a few of the weak features may be due to residual grain noise, the continuity from star to star of many weak features is evident. Two stars, μ Nor and ρ Lup, are also shown in Fig. 2.

Appendix B

SKYLAB ULTRAVIOLET STELLAR SPECTRA: THE WOLF-RAYET STARS

The Astrophysical Journal, Vol. 199, No. 3, Part 2, 1975 August 1

THE ASTROPHYSICAL JOURNAL, 199:L173–L175, 1975 August 1

SKYLAB ULTRAVIOLET STELLAR SPECTRA: THE WOLF-RAYET STARS

K. G. HENIZE, J. D. WRAY, S. B. PARSONS, AND G. F. BENEDICT
Department of Astronomy, University of Texas at Austin
Received 1975 March 13; revised 1975 April 18

ABSTRACT

Ultraviolet spectra showing emission lines in the 1300–2000 Å region have been obtained of 12 Wolf-Rayet stars. In the WN stars, lines of He II are dominant although N IV λ1718 and N III λ1805 are also present. C IV λ1549 absorption and a strong continuum in HD 151932, HD 93131, HD 92740 and HD 190918 indicate that all four stars have companions. In the WC stars, lines of C III and C IV dominate. N IV λ1718 and N III λ1805 emissions are probably present in HD 165763 and HD 156385. The ultraviolet spectra of γ Vel and θ Mus are dominated by supergiant companions.

Subject headings: spectra, ultraviolet — Wolf-Rayet stars

I. INTRODUCTION

Ultraviolet spectra in the region from 1300 to 5000 Å have been obtained from *Skylab* with a 15-cm aperture objective-prism telescope (Henize *et al.* 1975). Good quality spectra have resolutions of 2, 12 and 42 Å at wavelengths of 1400, 2000, and 2800 Å respectively.

Of the 23 W-R stars brighter than $V = 9.0$ (Smith 1967), observations were obtained of 20 stars. Most of these spectra exhibit large attenuation of intensity in the far ultraviolet, especially in the 2200 Å region, due to interstellar (and possibly circumstellar) extinction. Twelve stars (6 WN and 6 WC) show emission lines at wavelengths of 2000 Å or less, and it is those spectra which are discussed in this *Letter*. Calibrated flux measurements will be reported in a later paper.

II. THE WN STARS

Spectra of six WN stars are illustrated in Figure 1 (Plate L12), and a tabulation of the lines seen is presented in Table 1. The emission intensities given in Tables 1 and 2 are relative values measured on microdensitometer tracings and corrected approximately for the instrumental response. In the case of absorption lines the equivalent width is given in angstroms. The wavelengths given are laboratory wavelengths. Our wavelength identifications are based primarily on the published data of Smith (1972) and of Stecher (1970). Wavelengths for unidentified lines, in brackets, are measured relative to the easily identified lines with an accuracy which varies from about ±10 Å at 2000 Å to ±40 Å at 3000 Å.

Emission lines of He II dominate the ultraviolet region of these stars. The He II line at λ1640 is the strongest line shortward of 2000 Å, and the n^2F^o–3^2D series of He II is conspicuous in the 2000–3200 Å region. The prominance of He II in WN stars is also evident in infrared spectra (Kuhi 1968). The only other strong lines (except for C IV λ1549 discussed below) are N IV λ1718 and N III λ1805. Weak unidentified lines appear at λλ3000 and 2605.

TABLE 1

ULTRAVIOLET OBSERVATIONS OF WN STARS

λ (Å)	Ion	HD 190918	191765	192163	151932	93131	92740
1403 A.....	Si IV	...	...	...	...	3?Å	...
1403 E.....	Si IV	...	...	...	...	2?	3?
1549 A.....	C IV	...	...	...	...	4Å	(2)Å
1549 E.....	C IV	1?	...	...	2	(6)	(2)
1640 E.....	He II	(8)	(10)	8	5	6	...
1718 E.....	N IV	...	...	3	6	8	...
1805 E.....	N III	...	...	1	...	...	...
2385 E.....	He II	...	1	3	...	...	...
2512 E.....	He II	...	3	4	...	...	...
[2605] E.....	...	...	0+	1	...	...	...
2734 E.....	He II	...	6	6	...	...	...
[3000] E.....	...	...	1	4	...	...	...
3204 E.....	He II	...	9	20	...	...	...
3482 E.....	N IV	...	5	8	...	...	...
Classification:							
Smith (1967).....		WN4.5+O9.5 Ia	WN6	WN6	WN7	WN7	WN7
Revision.....		...	...	...	+O-B1 I	+O-B1 I	+O-B1 I

NOTE.—( ) = estimated; A = absorption line; E = emission line.

There appears to be a strengthening of the He II λ1640 line with earlier spectral type. Whereas this line is slightly weaker than N IV λ1718 in the WN7 stars, it is distinctly brighter in the WN6 stars.

Carbon λ1549 emission with shortward-displaced absorption is present in HD 93131 and HD 92740. Strong C IV absorption is not expected in WN stars; C IV λλ5801, 5812 emission is strong but does not show absorption components in WN stars (Underhill 1968). The C IV λ1549 profile and suspected Si IV λλ1394, 1403 emission are typical of early-type supergiants (Morton 1967; Henize *et al.* 1975), and it seems reasonable to attribute these features primarily to companion stars. Finally, a strong ultraviolet continuum is present which washes out the other emission lines in these spectra, further indicating the presence of hot companions. Underhill (1968) has suspected the presence of companions to both of these stars, Moffat and Haupt (1974) have suspected a companion to HD 93131, and Niemelä (1973) has demonstrated that HD 92740 is a spectroscopic binary. Our estimated spectral types for the companions are given in Table 1.

HD 151932 also shows C IV λ1549 emission and a continuum which is strong relative to the emission lines, evidence that this star also has a previously unknown companion. The fact that the only WN star in this group with a known companion, HD 190918, shows a strong continuum and suspected C IV emission also supports the above conclusions.

III. THE WC STARS

Spectra of six WC stars are illustrated in Figure 2 (Plate L13), and a tabulation of the lines seen is presented in Table 2.

Emission lines of C III and C IV are the dominant features in the ultraviolet spectra of the WC stars. Except for λ3204 and possibly λ2734, the n^2F^o–3^2D series of He II is not visible. The behavior of the λ3204 line is peculiar; it is strong in the WC8 star HD 192103 but is very weak in the WC5 star HD 165763.

The presence of weak to moderate emission lines near λλ1718 and 1803 indicate the possible presence of N IV and N III in HD 156385. The N IV λ1718 line is also suspected in HD 165763 and HD 152220 and is present in Stecher's (1970) scan of γ Vel. No satisfactory alternate identifications have been found for these lines. Although Si IV and Si II lines fall nearby, they are not expected to have significant strength in WC stars. Underhill (1968) has suspected the presence of nitrogen emission in several WC stars, but it is generally blended with carbon lines (Kuhi 1968). Since N IV λ1718 is the strongest line in the N IV spectrum longward of 1000 Å, its presence or absence should give a definitive answer to the presence of N IV lines in WC stars. Spectra in which wavelength can be measured accurate to ±1 Å should remove all doubt about the matter.

In Figure 2 the differences between the ultraviolet spectra of θ Mus and HD 156385 are interesting. HD 156385 shows strong emission lines standing out above a weak continuum, as is expected for W-R stars, while θ Mus shows a strong continuum in which the most outstanding features are C IV λ1549 and Si IV λλ1394, 1403 lines showing the marked P Cygni profiles typical of early-type supergiants (Henize *et al.* 1975). Closer inspection of θ Mus shows very weak emission at C III λλ2297, 1909 and of He II λ1640. It is clear that the ultraviolet spectrum is dominated by the O9.5 I companion and that the W-R emission lines barely show through its continuum. Considering the strengths of both its emission and absorption compo-

TABLE 2

ULTRAVIOLET OBSERVATIONS OF WC STARS

λ(Å)	Ion	Alternate Ion	HD 165763	θ Mus	156385	152270	γ Vel	192103
1335 A.....	C II	...	...	...	...	...	2 Å	...
1335 E.....	C II	...	...	...	...	...	85	...
1394 A.....	Si IV	...	...	(7) Å	...	...	7 Å	...
1403 A.....	Si IV						5 Å	...
1403 E.....	Si IV	...	...	(7)	(6)	...	65	...
1549 A.....	C IV	...	...	13 Å	6 Å	...	4 Å	...
1549 E.....	C IV	...	12	14	45	...	40	...
1640 E.....	He II	1645 C III	2	3	30	5	...	...
1655 E.....	C IV	1657 C I	...	...	7	...	...	...
1718 E.....	N IV	1724 Si IV	0+	3	12	3	...	...
1805 E.....	N III	1812 Si II	1	...	7	...	...	...
1909 E.....	[C III]	1908 N III	7	3	33	14	...	(2)
[2005] E.....	...	...	3	...	4	...	...	...
2297 E.....	C III	...	21	4	36	14	...	7
2406 E.....	C IV	...	8	...	8	...	...	3
2530 E.....	C IV	2524 C IV	21	6	33	...	...	9
2614 E.....	C III	2595 C IV	(2)	...	...	...	...	2
[2920] E.....	C IV?	...	(2)	...	...	...	...	4
3204 E.....	He II	...	2	...	...	...	...	10
3410 E.....	O IV	...	10	...	...	...	...	5
Classification:								
Smith (1967).....			WC5	WC6+O9.5 I	WC7	WC7+O5–8	WC8+O7	WC8 (+OB)
Revision.....			...	...	...	...	+B0:Ip	...

nents, it seems probable that the C IV λ1549 line arises mainly from the O9.5 star. This then raises a question as to the origin of the strong λ1549 absorption in HD 156385 which is not typical of any of the other lines in its ultraviolet spectrum. The λ1549 absorption is quite pronounced, as opposed to absorption components of lines such as C IV λλ5801, 5812 sometimes evident in visible spectra of WC stars (cf. Underhill 1968). Although this suggests the presence of a companion star, the lack of a strong continuum in the 1500–3000 Å region does not. Perhaps it is possible for resonance lines of appropriate ions in the W-R envelope to produce strong absorption as well as emission. The definition of the intrinsic spectrum of a Wolf-Rayet star, separated from any possible effects due to a companion, remains an interesting problem for further study.

The ultraviolet spectrum of γ Vel is also dominated by its companion star. The main features are strong lines of C IV, Si IV, and C II, all of which show conspicuous P Cygni profiles. Weak lines longward of λ1550 which were recorded by Stecher (1970) are lost in the overexposure of the strong continuum. The visual appearance of the C IV and Si IV lines is very similar to that of ϵ Ori (B0 Ia). Both the relative weakness of C IV compared with Si IV and the comparative sharpness of the Si IV absorptions indicate a spectral type later than O9.5 (see Henize *et al.* 1975). The strength of Si IV leaves no doubt of the supergiant character. However, the presence of C II λ1335 emission is anomalous since this emission is not visible in other O or B supergiant stars. Thus the ultraviolet spectrum must be classed as peculiar. The best classification to be derived from these data is B0: Ip which is to be compared with visual wavelength classifications of O7 (Smith 1967) and O9 I (Conti and Smith 1972).

In both γ Vel and θ Mus it is evident that the continuum of the companion dominates in the ultraviolet whereas the W-R radiation dominates the visible part of the spectrum. Thus both W-R stars must be cooler than their companions. In θ Mus the W-R energy distribution must be slightly cooler than that of an O9 supergiant, and an effective temperature on the order of 31,000 K or less is indicated. In γ Vel, if we accept the B0: I class derived for the companion from the Si IV and C IV lines, then a temperature of 28,000 K or less is indicated for the W-R component. This is significantly cooler than the value of 32,500 ± 2500 K derived by Code *et al.* (1975) and suggests either that the ultraviolet spectrum of the companion is too peculiar to allow a temperature-related classification or else that special effects in the extended atmosphere of the W-R component result in an attenuation of its ultraviolet radiation. For example, Mihalas and Hummer (1974) find an intrinsic reddening of the energy distribution of a hot extended atmosphere relative to a corresponding plane-parallel atmosphere. On the other hand Castor, Abbott, and Klein (1975) find that an extensive electron-scattering envelope will redden the light little, if any, but will measurably increase the apparent angular diameter.

Two unidentified lines appear in the WC stars, one at 2005 Å and the other 2920 Å. The λ2920 line is very weak, but λ2005 is easily visible and appears considerably enhanced in the spectrum of the WC5 star HD 165763. This suggests it may be a good indicator of temperature in the WC stars.

This work has been supported at the University of Texas under NASA contract NAS 9-13176.

REFERENCES

Castor, J. I., Abbott, D. C., and Klein, R. I. 1975, *Ap. J.*, **195**, 157.
Code, A. D., Davis, J., Bless, R. C., and Hanbury Brown, R. 1975, *Ap. J.*, in press.
Conti, P. S., and Smith, L. F. 1972, *Ap. J.*, **172**, 623.
Henize, K. G., Wray, J. D., Parsons, S. B., Benedict, G. F., Bruhweiler, F. C., Rybski, P. M., and O'Callaghan, F. G. 1975, *Ap. J.*, **199**, in press.
Kuhi, L. V. 1968, *Wolf-Rayet Stars* (NBS SP. 307), p. 103.
Mihalas, D., and Hummer, D. G. 1974, *Ap. J. Suppl.*, **28**, 343.
Moffat, A. F. J., and Haupt, W. 1974, *Astr. and Ap.*, **32**, 435.
Morton, D. C. 1967, *Ap. J.*, **147**, 1017.
Niemelä, V. S. 1973, *Pub. A.S.P.*, **85**, 220.
Smith, L. F. 1967, *M.N.R.A.S.*, **138**, 109.
———. 1972, in *Scientific Results from OAO-2*, ed. A. D. Code (Washington: NASA SP-310), p. 429.
Stecher, T. P. 1970, *Ap. J.*, **159**, 543.
Underhill, A. B. 1968, *Wolf-Rayet Stars* (NBS SP.-307), p. 183.

K. G. Henize: NASA/Johnson Space Center, Code TE, Houston, TX 77058

J. D. Wray, S. B. Parsons, and G. F. Benedict: Department of Astronomy, University of Texas, Austin, TX 78712

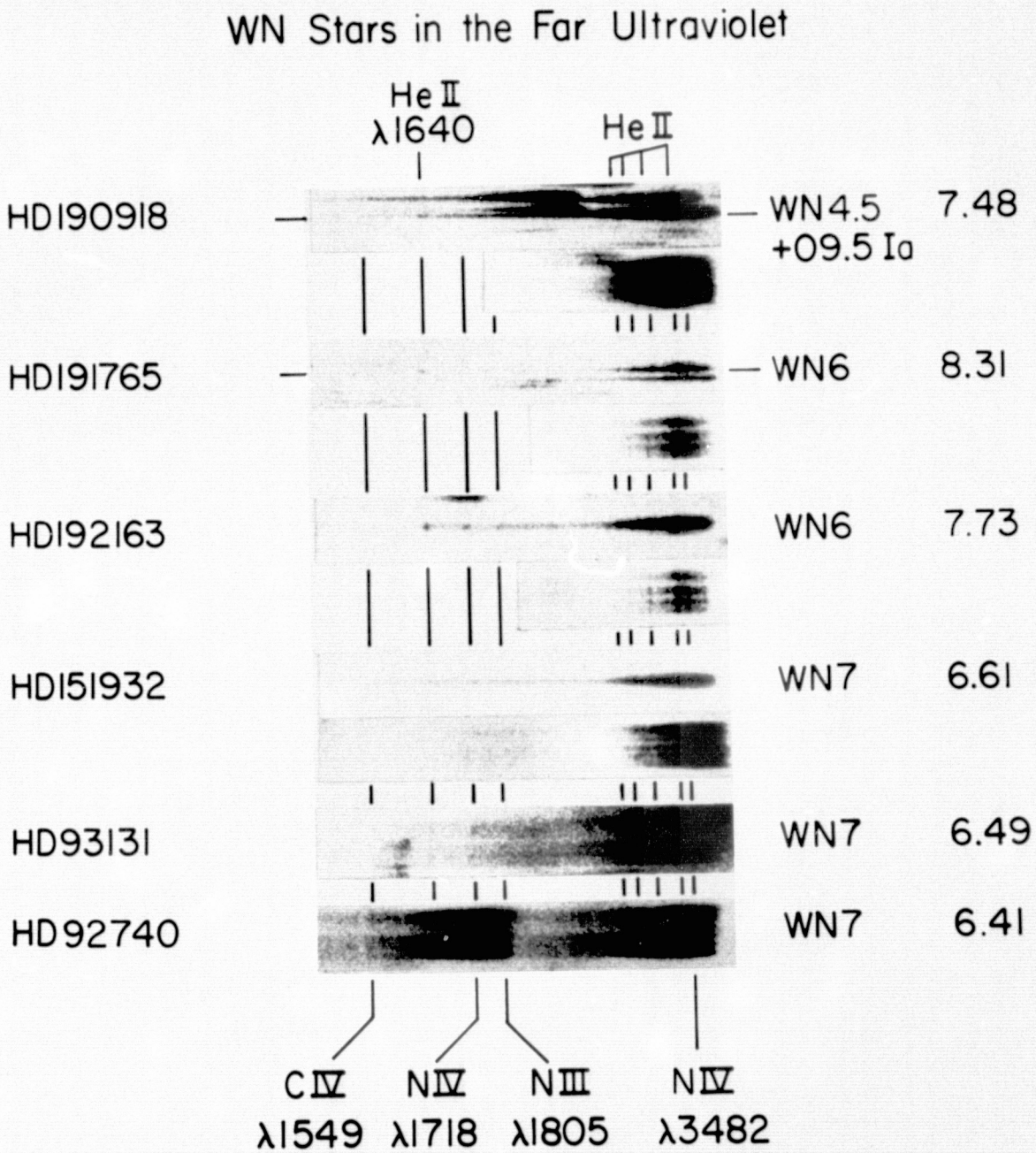

FIG. 1.—Ultraviolet objective-prism spectra of six WN stars. Note the C IV absorption and presence of continuum, pronounced in HD 92740 and HD 93131 and also detectable in HD 151932 and HD 190918, indicative of companion stars (see text). The spectral types given are from Smith (1967).

HENIZE *et al.* (*see* page L173)

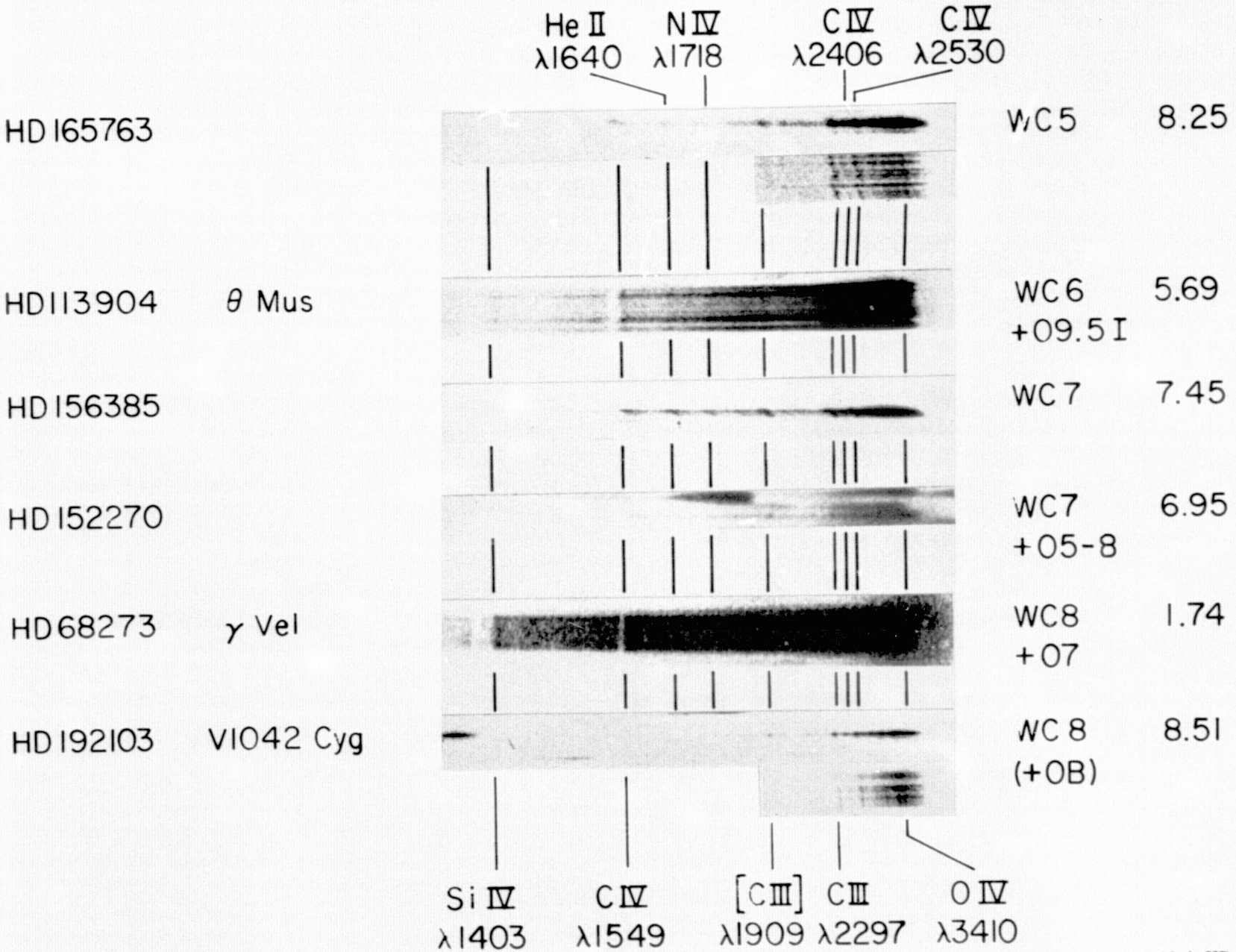

FIG. 2.—Ultraviolet objective-prism spectra of six WC stars. Spectral classifications are from Smith (1967). N IV appears to be present in several of these stars, notably in HD 156385.

Appendix C

ULTRAVIOLET Si IV/C IV RATIOS FOR Be STARS

Presented at IAU Symposium No. 70 September 1975

Symposium proceedings in press

Appendix C

ULTRAVIOLET Si IV/C IV RATIOS FOR Be STARS

Karl G. Henize*†, James D. Wray†, S. B. Parsons† and G. F. Benedict†

Abstract

The intensities of the very strong lines of C IV λ1549 and Si IV λλ1394, 1403 observed in spectra obtained with Skylab experiment S019 provide a sensitive discrimination of spectral type between B0 and B2. Eye estimates of the Si IV/C IV ratio are tabulated for 33 B0-B2, class III-V stars of which 11 are emission-line stars. Seven of the emission-line stars show significantly smaller ratios than normal stars of the same MK class. The most outstanding examples are 60 Cyg, o Pup, η Cen, and ι Ara.

* Astronaut Office, Code TE, NASA Johnson Space Center

† Department of Astronomy, University of Texas at Austin

I. Introduction

During this symposium Dr. Slettebak has already reviewed reasons why it is difficult to assign firm MK classes to the rapidly rotating Be stars, and Dr. Heap has noted how data on ultraviolet C IV and Si IV line intensities may be useful in providing improved classifications of such stars. This subject has also been on our minds as we carry out the analysis of UV spectra obtained with Skylab experiment S019. A preliminary survey of the behavior of the C IV and Si IV lines in early type main sequence stars (Henize et al. 1975) shows that the Si IV/C IV ratio varies dramatically from a value of about 10 at B2 to a value of about 1/4 at B0. This paper presents a more detailed study of the variation of the Si IV/C IV ratio as a function of spectral type for 33 B0-B2 stars of which 11 are Be stars.

II. The Observations

The instrumentation with which these data were obtained is described by Henize et al. (1975) and by O'Callaghan et al. (1976). The basic instrument is an objective-prism spectrograph with a 15-cm aperture and a 4° prism of CaF_2 giving resolutions of 2A and 12A at wavelengths of 1400 and 2000A respectively.

A total of 400 spectra showing measurable fluxes at 1500A have been obtained and, of these, roughly 120 show evident absorption or emission lines.

Although these spectra are calibrated so that equivalent widths and flux curves may be derived, all factors entering the calibration are not yet completely analyzed and, as a consequence, the data presented here are based on eye estimates of absorption line intensities. These estimates are affected by the differing dispersions and effective exposures of 1400A vs. 1550A and it is not to be expected that they will correspond to ratios of the equivalent widths. Nevertheless they represent a self consistant set of data from which stars showing anomalous behavior may be detected.

Initially, spectra of all stars with spectral types B0-B2 and luminosity classes III - V which showed visible flux at 1400A were examined. This list of 98 stars yielded 34 stars for which both the C IV and Si IV lines are well-exposed and in which reasonably reliable line intensities can be determined. These stars and their Si IV/C IV ratios are listed in table 1. Since the Si IV doublet is well resolved in our spectra and the C IV doublet is not, the ratio given is defined as Si IV λ1394/C IV λλ1548, 1551. The spectral types in table 1 are derived from Hiltner et al. (1969) and Lesh (1968).

III. Discussion

The data of table 1 are displayed in figure 1. For the non-emission-line stars there is a clear cut trend for the Si IV/C IV ratio to increase from about 1/5 at B0, through 4 at B1, to roughly 8 or 10 at B2. The emission-line stars, on the other hand,

Appendix C

Table 1

Si IV λ1394/C IV λλ1548, 1551 Ratios for B0-B2 Stars

HD	Desig.	Sp.	Si IV/C IV	Remarks
3360	ζ Cas	B2 IV	1/2	C IV very strong for B2
5394*	γ Cas	B0.5 IVe	1	
10516*	φ Per	B2 Vep	>2	Si IV very weak
34816	λ Lep	B0.5 IV	3/4	
35468	γ Ori	B2 III	10	
36512	υ Ori	B0 V	1/8	
36822	φ^1 Ori	B0.5 IV-V	1/4	
50013*	κ CMa	B1.5 IVne	>4	
58978*	HR 2855	B0.5 IVnpe	<1/4	
63462*	o Pup	B1 IV:nne	1/3	
75821	HR 3527	B0 III	1/6	
79351	a Car	B2 IV-V	>4	
93030	θ Car	B0.5 Vp	2	C IV very weak for B0.5
108248	α^1 Cru	B0.5 IV	4	with α^2 Cru B1 V
116658	α Vir	B1 IV	4	
120640	HR 5206	B2 Vp	>6	
120991*	HR 5223	B2 IIIe		Si IV very weak for B2
127381	σ Lup	B2 III	5	
127972*	η Cen	B1.5 Vn	2	
132058	β Lup	B2 III	>6	
132200	κ Cen	B2 IV	>6	
135160*	HR 5661	B0.5 V	1/2	
143018	π Sco	B1 V+B2	10	
147165	σ Sco	B1 III	4	
149438	τ Sco	B0 V	1/3	
151890	μ^1 Sco	B1.5 IV	4	
157042*	ι Ara	B2 IIIne	1:	UV spectrum unwidened
158408	υ Sco	B2 IV	6	
158926	λ Sco	B1.5 IV	10	
173948*	λ Pav	B2 II-III	1:	Si IV very weak; C IV broad, Fe III?
188439	V819 Cyg	B0.5 IIIp	1/2	1600-2000 blends strong
200310*	60 Cyg	B1 Vne	1/2	
214168*	8 Lac	B1 Ve	1:	with HD214167 B1.5V; C IV broad, Fe III?
224572	σ Cas	B1 V	4	

* Emission-line star

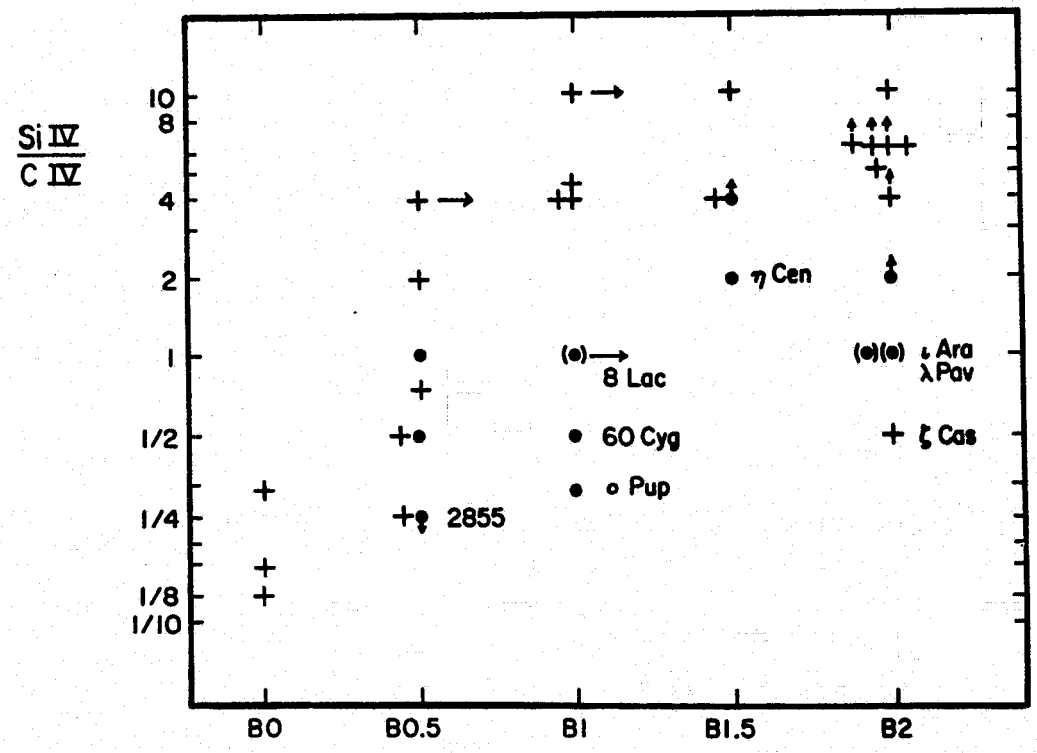

Figure 1. The Ratio Si IV 1394/C IV λλ1548, 1551 Plotted as a Function of Spectral Type. Crosses indicate non-emission-line stars; dots indicate emission-line stars. Parentheses indicate uncertainty in the Si/C ratio. ↑ indicates values which are lower limits of the ratio. → indicates that the spectrum is blended with one of slightly later type.

show generally smaller ratios that the non-emission-line stars. In particular, seven of the eleven emission-line stars show ratios significantly less than those for normal stars. Of these, four stars (60 Cyg, o Pup, η Cen and ι Ara) have a C IV intensity conspicuously greater than that of the normal stars of the same spectral class. Two of the remaining stars, λ Pav and HR 2855, are peculiar in that the Si IV lines are unusually weak for their spectral class. This peculiarity is also evident in φ Per and HR 5223.

For the four stars in which C IV is enhanced the data in figure 1 suggest that they are hotter than the MK classes indicate. The rough calibration of the Si/C ratio provided in figure 1 suggests spectral classes of B0.2, B0.5, B0.5 and B0.7 for o Pup, 60 Cyg, ι Ara and η Cen respectively assuming them to be main sequence stars. However, the Si/C ratio is also correlated to luminosity and at spectral class B1 the ratio ranges from about 0.1 for main sequence stars to about 1 for supergiant stars (see figure 3d of Henize et al. 1975). Thus the enhancement of C IV may also be due to a lower than expected surface gravity. The Si/C ratio in 60 Cyg, for example, is also compatible with a classification of B1 II. Since these stars may be expected to show incipient shell absorption and since shell spectra generally show high luminosity characteristics, this is the more attractive of the two possibilities.

The suggestion that the enhancement of C IV absorption may be due to an incipient absorption shell leads to the further question as to whether these four stars show any indication of the extensive

blends of weak lines in the 1600-2000A region which are evident in spectra of the advanced shell stars 48 Lib and ζ Tau and also in many of the O and early B supergiants (see figure 3a, Henize et al. 1975). A weak indication of such lines is present in o Pup and 60 Cyg but in ι Ara and η Cen this region of the spectrum is over-exposed. It should be noted in passing that these blended shell (or supergiant) absorption features are strong in the star V819 Cyg. There is also a suspicion of weak emission present on the redward edge of C IV. Thus the UV spectrum of V819 Cyg is more like that of a B0 or B1 supergiant than that of a B0.5 III star.

The star ζ Cas also shows enhanced C IV even though it is not an emission-line star. The spectral class suggested by the Si/C ratios in figure 1 is B0.5. The peculiarity of ζ Cas is further accentuented by the fact that it is an MK standard (Morgan and Keenan 1973). The C IV anomaly brings into question whether or not this star is a reliable standard star and further investigation of abundances in this star would seem to be warranted.

One further possibility for explaining C IV enhancement should be mentioned; i.e. the possibility that the C IV line is severely blended with Fe III as is suggested by Peytremann (1975) for all stars cooler than 30000°K. However, in the five stars discussed above the C IV absorption is sharp and distinct and there is little doubt that it is attributable to C IV. A broad blending of weak lines in the 1500 to 1600A region which probably corresponds to the blend studied by Peytremann is visible in many B1 and B2 stars on our plates, but at the resolution of the S019 spectra, it is not easily

confused with the C IV line. The question as to why the empirical data do not agree well with theory is a matter of interest and will be the subject of further study in the S019 spectra.

Two stars in table 1, λ Pav and 8 Lac, do show a somewhat diffuse C IV line and in this instance it might be suspected that the feature is seriously blended with Fe III. If so, then their Si/C ratio is somewhat greater than is indicated in figure 1. This would remove both stars from the anomalous group of stars so far as the Si/C ratio is concerned. However, the fact that λ Pav (together with HR 2855, φ Per, and Hr 5223) shows abnormally weak Si IV bears further consideration. Inspection of figure 3 of Henize et al. (1975) suggests that the UV spectra of these stars are more like those of B3 stars in which the Si IV and C IV have almost completely disappeared. The reason for such a trend of misclassification is difficult to understand, however, since in rapidly rotating stars the main effect is to obscure the weak lines required to establish a class of B0 or B1 and to enhance the strength of He. Both effects tend to lead to classification of B2 and B3 for rapid rotators even though they may be considerably hotter.

References:

Henize, K. G., Wray, J. D., Parsons, S. B., Benedict, G. F., Bruhweiler, F. C., Rybski, P. M., and O'Callaghan, F. G. 1975, Ap. J. Letters, 199, L119.

Hiltner, W. A., Garrison, R. F., and Schild, R. E. 1969, Ap. J., 157, 313.

Lesh, J. R. 1968, Ap. J. Suppl., 17, 371.

Morgan, W. W., and Keenan, P. C. 1973, Ann-Rev. Astr. and Ap., 11, 29.

O'Callaghan, F. G., Henize, K. G., and Wray, J. D. 1976, Applied Optics, in press.

Peytremann, E. 1975, Astr. and Ap., 39, 393.

Appendix D

SKYLAB ULTRAVIOLET STELLAR SPECTRA: EMISSION LINES FROM THE BETA LYRAE SYSTEM

Submitted to The Astrophysical Journal November 21, 1975

Appendix D

SKYLAB ULTRAVIOLET STELLAR SPECTRA: EMISSION LINES FROM THE BETA LYRAE SYSTEM

Y. Kondo,* S. B. Parsons,† K. C. Henize,*† J. D. Wray,†
G. F. Benedict,† and G. E. McCluskey‡

Received _____

ABSTRACT

Observations of β Lyr with the Skylab S-019 ultraviolet objective-prism spectrograph show numerous emission lines in the region 1400-2300 Å. Some variations in line strength between phases 0.25 and 0.50 are seen, which probably explain the shallowness of the OAO-2 light curve at 1910 Å. Many of the emission lines are found to be intercombination transitions, thus confirming the concept that the emission is produced by collisional excitation in low-density clouds of hot gas.

Subject headings: stars: eclipsing binaries -- ultraviolet: spectra

* Johnson Space Center, Houston

† Department of Astronomy, University of Texas at Austin

‡ Lehigh University, Bethlehem

I. INTRODUCTION

The close binary system β Lyr is currently undergoing a shortlived phase (10^3 to 10^4 years) of dynamic mass transfer during which the primary component is believed to be losing mass at the rate of 10^{-5} to 10^{-6} $m_\odot$ per year. The primary component is classified as a B8 to B9 object based on the visible spectrum. The spectrum of the secondary component has not been detected in any spectral region. The mass function derived from the spectroscopic observations of the primary is 8.5 $m_\odot$ (Struve 1958). Although the mass function sets a minimum value for the mass of the secondary at 8.5 $m_\odot$, a value well above 10 $m_\odot$ is probable. The invisibility of the spectrum of a star with such a large mass has long puzzled students of this binary. For recent discussions of this fascinating object, we refer the reader to Kriz (1974), Hack et al. (1975) and Kondo, McCluskey and Eaton (197_).

The first ultraviolet observations of β Lyr were obtained with the photometer of the OAO-2 Wisconsin Experiment Package (Houck 1971; Kondo, McCluskey and Houck 1971). Studies of the light curve at several ultraviolet wavelengths gave the surprising result that the depth of secondary eclipse increased as wavelength decreased. A further puzzle appeared in the 1910Å band (filter half-width = 260Å) where both eclipses were shallower than at any other wavelength. Copernicus high resolution spectra shortward of 1500 Å (Hack et al. 1975) showed that the far-ultraviolet spectrum of β Lyr is completely dominated by the low excitation emission lines of multi-ionized atoms. The ultraviolet spectrum of β Lyr is not at all like a late B-type star, and is, in fact, unlike any other object observed with Copernicus

or with the Skylab S-019 spectrograph. Recently, Hack (1974) reported lower resolution (35 Å) observations of this binary with the S2/68 experiment onboard the TD-1 satellite and suggested line identifications in the 1400-2500 Å spectral range.

The present paper reports spectroscopic data in the 1300-2500 Å wavelength region obtained with the Skylab S-019 ultraviolet objective-prism spectrograph. Ground-based spectrograms taken at about the same time are also described.

II. OBSERVATIONS

Three spectra of β Lyr were obtained during the second Skylab mission with the S-019 spectrograph. This instrument (see Henize et al. [1975b] for a more complete description) has a 15 cm aperture and achieves a wavelength resolution of 2, 12 and 42 Å at 1400, 2000 and 2800 Å respectively. Exposure data for the β Lyr spectra are given in Table 1.

The competition for observing time on Skylab and the basic survey objective of experiment S-019 made it impossible to obtain more than a few spectra of this particular star. Therefore a special effort was made to obtain observations during secondary eclipse (phase 0.5) and midway between eclipses (phase 0.25). Moreover, it was possible also to schedule two of the exposures (SL3-230 and SL3-263) to be simultaneous with Copernicus observations.

Figure 1 illustrates relative intensity traces of the three plates of β Lyr, compared with ρ Leo (B1 Iab) and HD 156385 (WC7). The intensities, based on preliminary characteristic curves, represent intensity per unit wavelength but are not corrected for instrumental transmission and film sensitivity. The abscissae are proportional to plate position and therefore the wavelength scale is characterized by the prismatic dispersion function. Our wavelength identifications are based on rocket spectra for early B-type stars (Morton et al. 1972) and for the solar chromosphere (Burton and Ridgeley 1972), with the aid of the tables by Moore (1950, 1970) and by Kelly and Palumbo (1973). Interpolation among known lines is accomplished with averaged residuals from a Hartmann formula; this results in a relative wavelength scale accurate to ± 1 Å at 1500Å and ± 3 Å at 2000Å. It is not always possible

TABLE 1

TIME OF OBSERVATIONS

Plate No.	Date & Time Exposure Started (1973)	Exposure	Phase	Remarks
SL3-034	Aug. $10^d 21^h 52^m 54^s$	227^s	0.25	Well exposed from 1320 to 1900 Å. Overlap from 1560 to 1700 Å.
SL3-230	Sep. $5^d 14^h 41^m 08^s$	956^s	0.25	Well exposed from 1540 to 1900 Å. Overlap from 1540 Å shortward.
SL3-263	Sep. $21^d 09^h 56^m 32^s$	232^s	0.50	Well exposed from 1500 to 2300 Å.

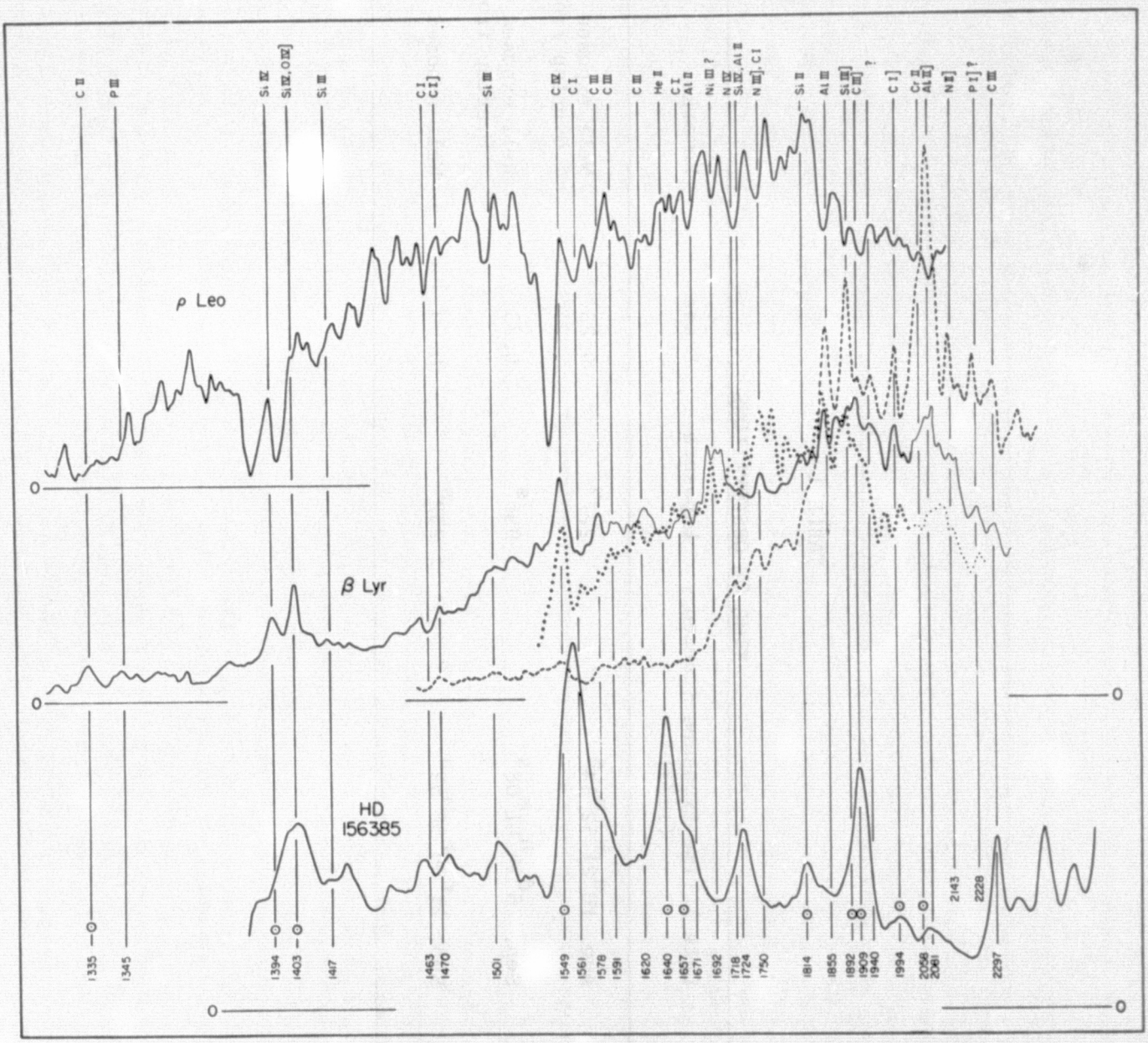

Figure 1. Relative Intensities in the Rectified Spectra of β Lyr, ρ Leo (B1 Iab), and HD 156385 (WC7). The three exposures of β Lyr are plotted with the same zero-point: _____ SL3-034; ..... SL3-230; ----- SL3-263. Regions of slight overexposure or overlap are indicated by thinner curves. Suggested line identifications are indicated; strong emission lines in the solar chromospheric spectrum are marked with "Θ".

to line up different traces perfectly, due to small second-order changes in the dispersion function with field position. Thus some of the apparent wavelength shifts in Figure 1 may not be related to Doppler shifts.

Several conspicuous emission features shortward of 2200Å are listed in Table 2. Less prominent features which appear in at least two of the three spectra are listed separately in Table 3. The line identifications given are frequently at variance with those of Hack (1974) which were based on lower resolution data. After noting several coincidences between strong emission lines in the solar chromosphere and emission features in β Lyr, we gave high weight to chromospheric lines in making the identifications. In general, preference was given to lines of the lighter elements lying closest to the measured wavelengths. We found that a large fraction of the mid-ultraviolet emission lines in β Lyr are most reasonably identified as due to intercombination ("semi-forbidden") transitions.

Two interesting characteristics in the behavior of the emission lines should be noted. Although each plate has a restricted wavelength range in which reliable spectrophotometry can be carried out, some real differences are seen in the line strengths. First, the C IV doublet around 1550 Å is probably weaker at phase 0.5 than at phase 0.25. This variation agrees with the Copernicus observations at wavelengths shortward of about 1420 Å, which showed that the emission lines are generally weaker at phase 0.5. Second, some of

TABLE 2

PROMINENT EMISSION LINES

Wavelength (Å)	Identification	Term	Upper State E.P. (ev)	Ratio of emission at Phase 0.5 to Phase 0.25
1335	C II (1335.71, 34.53)	$2p\ ^2P^\circ - 2p^2\ ^2D$	9.3	-
1394	Si IV (1393.76)	$3s\ ^2S - 3p\ ^2P^\circ$	8.9	-
1403	Si IV (1402.77)	$3s\ ^2S - 3p\ ^2P^\circ$	8.8	-
	O IV multiplet	$2p\ ^2P^\circ - 2p^2\ ^4P$	8.8	-
1549	C IV (1548.18, 50.77)	$2s\ ^2S - 2p\ ^2P^\circ$	8.0	(0.7)
1855	Al III (1854.72, 62.79)	$3s\ ^2S - 3p\ ^2P^\circ$	6.6	2.3
	C I (1855.4)	$2p^2\ ^1D - 2p^3\ ^3D^\circ$	8.0	
	(Fe II multiplet 7)			
	(Fe III multiplet 63)			
1892	Si III (1892.03)	$3s^2\ ^1S - 3p\ ^3P^\circ$	6.6	2.1
	(Fe III multiplets)			
1994	C I (1993.62)	$2p^2\ ^1D - 3s\ ^3P^\circ$	7.5	(1.4)
	(Fe III multiplet 81)			
2081	Al II (2081.5, 87.0)	$3p\ ^3P^\circ - 3p^2\ ^1D$	10.6	(2.5)
	(Fe II multiplets)			
	(Fe III multiplet 48)			

TABLE 3

PROBABLE EMISSION FEATURES

Wavelength (Å)	Identification	Term	Upper State E.P. (ev)
1578	C III multiplet 12.03	$3d\ ^3D - 3d'\ ^3F^\circ$	41.3
1591	C III (1591.44)	$3s\ ^1S - 3s'\ ^1P^\circ$	38.4
1620	C III (1620.07, 20.33)	$3p\ ^3P^\circ - 4d\ ^3D$	39.9
1692	? Ni III (1692.51)	$a\ ^5F - z\ ^5G^\circ$	13.9
1750	N III (1748.61, 49.67)	$2p\ ^2P^\circ - 2p^2\ ^4P$	7.1
	N III multiplet 19	$2p^2\ ^2P - 2p^3\ ^2D^\circ$	25.2
	C I (1751.83)	$2p^2\ ^1S - 3d\ ^1P^\circ$	9.8
1909	C III (1908.73)	$2s^2\ ^1S - 2p\ ^3P^\circ$	6.5
1940	?		
2058:	Cr II multiplet 1	$a\ ^6S - z\ ^6P^\circ$	6.0
2143:	N II (2142.8, 39.0)	$2p^2\ ^3P - 2p^3\ ^5S^\circ$	5.8
2228:	? P I multiplet 3	$3p^3\ ^2D^\circ - 4s\ ^4P$	6.9
2297	C III (2296.9)	$2p\ ^1P^\circ - 2p^2\ ^1D$	18.1

On the Skylab plate of best quality, SL3-263, there is some indication of bifurcated emission lines. In the ground-based spectra, we see Hβ at 4861Å as bifurcated emission in both plates and no absorption component is seen. In the June 16 data from Kitt Peak, the shortward component is much weaker, while in the September 27 spectra both emission components are nearly equal in intensity. The He I λ4471 line appears with a P-Cygni profile in June; the same line observed in September appears as a rather complex feature with relatively weak emission at both ends and near the center of absorption. The same is true for Hδ. The He I line at 4025Å has a P-Cygni profile with a weak emission wing in June; in September, the longward emission is even weaker and there is a possible emission near the center of absorption. Whenever there is emission near the center of absorption, the absorption width itself becomes noticeably wider. The He I λ3888 line has a prominent P-Cygni profile in the June data; in September, the P-Cygni profile persists but with a weaker emission component on the shortward side of the emission as well. The He I line at 3819Å in June is essentially an absorption line with a suggestion of its being a very weak P-Cygni line; it has an appearance of a normal absorption line in September. The remaining Balmer lines shortward of Hδ appear as normal absorption lines in both plates. To summarize, in the June spectrum, the shortward emission is considerably weakened or non-existent, whereas, in the September spectrum, the shortward emission is present whenever the longward emission exists. The longward emission tends to be stronger in June than in September; in P-Cygni features, an emission is also present inside the absorption in the September spectrum and the absorption itself appears wider.

the emission lines in the vicinity of 1900Å, notably λ1855 and λ1892, are stronger at phase 0.5 than at phase 0.25. This will be discussed further below.

The general flux level drops rather abruptly shortward of about 1700 Å for phase 0.5 while no such decrease is seen at phase 0.25. Although some change in slope might be expected on the basis of the OAO-2 filter photometry for this binary (Kondo et al. 1971), most of the decreased intensity at shorter wavelengths on plate SL3-263 can be accounted for by the decreased reflectivity of the articulated mirror during the second Skylab mission. This is confirmed by the spectra of non-variable stars in the same field.

The C II λ1335 emission feature (Hack et al. 1975) which is irregularly variable in β Lyr (Bless and Eaton 1975) is clearly visible on plate SL3-034; the other plates are not usable in this region.

At least two absorption lines are found in the Skylab spectra of β Lyr. One at 1463 Å is probably due to a C I transition from a metastable state. The line at about 1565 Å, especially strong and broad on plate SL3-263, is not easily identified.

Ground-based spectra in support of the Skylab observations were obtained by Abt at the coudé focus of the 84-inch (2.1 m) telescope at Kitt Peak National Observatory. The exposures were made at the dispersion of 16.8 Å mm^{-1} covering the range from about 3500 to 5000 Å, on 1973 June $16^d6^h19^m-22^m$ and 1973 September $27^d2^h43^m-45^m$ (U.T.). The phases at the time of these observations were computed as 0.98 and 0.93, respectively. These phases as well as the phases given in Table 1 were derived from the recent light elements by Herczeg (1973).

III. DISCUSSION

It is not clear if these changes in spectral features in the coudé observations are due to the small differences in phases and/or to the changing pattern of the mass flow in β Lyr. (That is why we have preferred to refer to the data by date rather than by phase.) It does demonstrate that a turbulent gas motion on a massive scale is going on in this binary. Disappearance or weakening of shortward emission components at phase 0.98, which are present at phase 0.93, indicates stratification of the gas streaming and/or the presence of several emitting regions with different characteristic velocities. Such a picture of the circum-binary gas is basically in accordance with the ultraviolet results including the current study.

The broad absorption feature longward of the C IV λ1548, 1551 doublet at phase 0.5 might be interpreted as due to a stream rich in C IV moving away from the observer, perhaps re-entering the binary system in the line of sight to the primary. The center of this absorption is displaced from the emission peak by nearly 20Å implying that the velocity of the gas stream would be ≈4000 km s^{-1}. On the other hand, the feature might be due partly to C I λ1561. This would add to a complex pattern of C I absorptions and emissions which appear to be present in β Lyr: absorption at λ1463 flanked by emission at λ1470 and probably λ1459; possible time-dependent absorption or emission at λ1561; probable weak emission at λ1657 (strong in the solar chromosphere); and strong emission at λ1994.

Although the spectrum of β Lyr is unique, it is of interest to compare it with two classes of stars which have at least some of the lines in common; early B supergiants and WC stars. Therefore the S-019 spectra of ρ Leo and HD 156385 are displayed in Figure 1.

There is almost an inverse correlation between the spectra of ρ Leo and β Lyr; many absorption lines in the supergiant, notably λ1855 and λ1892 as well as the Si IV and C IV resonance lines, are found in emission in β Lyr. At the present resolution, however, we cannot be sure that the very same transitions are involved. For example, Fe III is probably more reasonable than C I] for the λ1994 absorption feature (which happens to be more prominent in the B1 Ib star ζ Per than in ρ Leo). The λ1892 feature is probably due to Si III] in the extended atmosphere of the supergiants as well as in the β Lyr system, since the lower state is the ground state. The C IV profile in ρ Leo indicates the rather strong mass outflow. The strong C IV emission in β Lyr confirms Copernicus observations indicating the existence of a substantial emitting region with a rather high degree of ionization.

The C III] λ1909 emission, strong in HD 156385 and requiring a gas density $\approx 10^{10}$ cm^{-3} or less (Osterbrock 1970), is possibly present in β Lyr with fairly constant intensity, while the nearby Si III] line changes strength. Also, He II λ1640 emission which is strong in the WC star is weak or absent in β Lyr, a surprising result, yet one which is consistent with the null result for He II λ1085 from Copernicus (Hack et al. 1976). C III λ 2297 is probably present in β Lyr at both phases. Some of the most definite coincidences between β Lyr and the WC star are weaker features not previously identified in the WC stars (Henize et al. 1975a). The λ1994 feature was listed by these authors with an estimated wavelength at 2005 Å. The strong emissions in β Lyr in the range 1994-2143 seem to be present in the WC star. Si III λ 1501 emission may be present both in β Lyr and in HD 156385. We note that the λ 1724 (Si IV) and λ1808-1817 (Si II) features in HD 156385 had been considered more likely due to

N IV λ1718 and N III λ1805 by Henize et al. (1975a). However, the S-019 wavelength calibration is now firm enough to suggest that the silicon identification is more likely than nitrogen. Si IV λ1724 or metastable Al II λ1725 may be in absorption in β Lyr; on the other hand, there may be emission from N IV λ1718.

The behavior of the emission lines in the vicinity of 1900Å appears to explain the unusual behavior of the OAO-2 light curves for β Lyr. The light curve at 1910Å shows a lesser amplitude than those at longer and shorter wavelengths (Kondo et al. 1971). It was speculated that the emitting gas clouds which contribute significantly to the total light of the system are located in the Lagrangian triangular points L_4 and L_5 (Kondo et al. 197_). If the light variation of β Lyr in the ultraviolet, at least shortward of about 2200Å, is due, to a significant extent, to the viewing angle effect of an emitting gaseous cloud surrounding the binary which may have the appearance of a dumb-bell or ellipsoid (Kondo and McCluskey 1974), additional clouds located at L_4 and L_5 can have the effect of making the eclipses shallower.

How do we explain the requirement that the gas clouds located at L_4 and L_5 emit mostly near 1910Å? After examining the second round of Copernicus observations obtained in 1974, Hack et al. (1976) conclude that the far ultraviolet emission lines are not radiatively excited but collisionally excited. Their results indicate localization of different emission lines which is interpreted as being due to the characteristic energy of electrons in a particular zone which may preferentially excite certain lines because of their optimized excitation cross-section. One may then speculate that those lines around 1910Å have excitation cross-sections that are optimized for the characteristic electron energy that prevails in the neighborhood of the L_4 and L_5 points.

The lines in this wavelength region represent somewhat lower ionization energies than the far ultraviolet lines identified in the Copernicus scans. Most of the strong solar chromospheric lines in the 1900Å region (the main exception being Si II λλ 1808, 1817) are present in β Lyr. Although the relative strengths are different, this suggests some similarity in electron densities, which are in the range 10^{10} - 10^{11} cm^{-3} in the solar transition region (Gingerich et al. 1971; Dupree 1972). The several intercombination transitions identified in the present study offer additional evidence that the energy levels are collisionally rather than radiatively excited. Most of the emission lines arise from levels lower than 20ev; if recombinations were significant in the gas around β Lyr, the high-excitation He II λ1640 (48 ev) and λ1085 (52 ev) emission should also be seen. Apparently the gas responsible for most of the lines seen in the Skylab spectra has densities ≈ 10^{10} cm^{-3} and mean energies ≈ 8 ev, with the ionizations being due to the high-energy tail of the electron velocity distribution.

IV. CONCLUSIONS

The ultraviolet spectra of β Lyr obtained at phases 0.25 and 0.5 from Skylab show that most of the emission lines near 1910Å are stronger at phase 0.5 than at phase 0.25. This is possibly because these emission lines arise from the clouds located around the Lagrangian triangular points, L_4 and L_5. This behavior of the emission in the vicinity of 1910Å explains the shallowness of the OAO-2 light curve at that wavelength. Collisional excitation of emission lines by electron streams with different characteristic

energies may give rise to segregation of various emission lines in the ionized gas surrounding this binary.

Moderate to high spectral resolution observations are needed at all possible wavelengths in order to continue to unravel the physical processes in the β Lyr system. The current observations were obtained only at phases 0.25 and 0.5. Observations in this spectral region (1400-2500Å) at other phases, especially at phases 0.0 and 0.75, are needed to verify the results presented in this report. Such observations are being planned with the International Ultraviolet Explorer (IUE) scheduled for launch in 1977.

We express our thanks to the Skylab II crew who obtained the observations for us and to the many personnel at Johnson Space Center who assisted in the flight planning and scheduling of these particular observations. We also wish to express our sincere appreciation to Dr. Helmut A. Abt for obtaining numerous coudé spectra in support of the Skylab S-019 observations. We thank Drs. G. Shields and D. Lambert for their comments on the manuscript. The S-019 data reduction and analysis at the University of Texas is supported by NASA contract NAS-8-31459.

REFERENCES

Bless, R. C., and Eaton, J. 1975, in talk at 146th A.A.S. meeting (Bull. AAS, 7, 405).*

Burton, W. M., and Ridgeley, A. 1970, Solar Phys., 14, 1.

Dupree, A. K. 1972, Ap.J., 178, 527.

Gingerich, O., Noyes, R. W., Kalkofen, W., and Cuny, Y. 1971, Solar Phys., 18, 347.

Hack, M. 1974, Astr. and Ap., 36, 321.

Hack, M., Hutchings, J. B., Kondo, Y., McCluskey, G. E., Plavec, M., and Polidan, R. S. 1975, Ap. J., 198, 453.

Hack, M., Hutchings, J. B., Kondo, Y., McCluskey, G. E., and Tulloch, M. K. 1976, Ap. J., submitted for publication.

Henize, K. G., Wray, J. D., Parsons, S. B., and Benedict, G. F. 1975a, Ap. J. (Letters), 199, L173.

Henize, K. G., Wray, J. D., Parsons, S. B., Benedict, G. F., Bruhweiler, F. C., Rybski, P. M., and O'Callaghan, F. G. 1975b, Ap. J. (Letters) 199, L119.

Herczeg, T. J. 1973, IAU Comm. 27 Bull., No. 828.

Houck, T. E. 1971, in Scientific Results from OAO-2, ed. A. D. Code (Washington: NASA SP-310), p. 479.

Kelly, R. L., and Palumbo, L. J. 1973, Atomic and Ionic Emission Lines Below 2000 Angstroms (Hydrogen through Krypton), NRL Rpt. 7599.

Kondo, Y., and McCluskey, G. E. 1974, Ap. J. (Letters), 188, L63.

Kondo, Y., McCluskey, G. E., and Eaton, J. 197_, Ap. and Space Sci., in press.

Kondo, Y., McCluskey, G. E., and Houck, T. E. 1971, in Scientific Results from OAO-2, ed. A. D. Code (Washington: NASA SP-310), p. 485.

Kriz, S. 1974, Bull. Astr. Inst. Czech., 25, 6.

---

* [the datum referred to was given in their oral presentation but not in their published abstract]

Moore, C. E. 1950, An Ultraviolet Multiplet Table, NBS Circ., No. 488, Sec. 1.

_____. 1970, Selected Tables of Atomic Spectra, Nat. Stand. Ref. Data Ser. — NBS, 3, Sec. 3.

Morton, D. C., Jenkins, E. B., and Macy, W. W. 1972, Ap. J., 177, 235.

Osterbrock, D. E. 1970, Ap. J., 160, 25.

Struve, O. 1958, Pub. A. S. P., 70, 5.

Y. KONDO: NASA/Johnson Space Center, Code TN23, Houston, TX 77058

G. T. BENEDICT, S. B. PARSONS, and J. D. WRAY: Department of Astronomy, University of Texas, Austin, TX 78712

K. G. HENIZE: NASA/Johnson Space Center, Code TE, Houston, TX 77058

G. E. McCLUSKEY: Department of Mathematics, Division of Astronomy, Lehigh University, Bethlehem, PA 18015

Appendix E

SKYLAB ULTRAVIOLET STELLAR SPECTRA: COOL STARS WITH HOT SECONDARIES

Astrophysical Journal (In Press) January 15, 1976

Appendix E

SKYLAB ULTRAVIOLET STELLAR SPECTRA: COOL STARS WITH HOT SECONDARIES

S. B. PARSONS*, J. D. WRAY*, Y. KONDO†, K. G. HENIZE*†, and G. F. BENEDICT*

Received May, 1975

ABSTRACT

A hot companion to the G5 III star HR 3080, a single-line spectroscopic binary, has been discovered from spectra in the vacuum ultraviolet. The companion must be a subdwarf or pre-white dwarf. A list of previously known ζ Aur- and VV Cep-type systems observed with the ultraviolet spectrograph on Skylab is also given.

Subject headings: spectroscopic binaries--subdwarfs--white dwarf stars--spectra, ultraviolet--stars, individual

*Department of Astronomy, University of Texas at Austin

†Johnson Space Center, Houston

I. INTRODUCTION

An objective prism survey of 9% of the sky to wavelengths as short as 1300Å was carried out during the three Skylab missions. The instrumentation and representative spectra for stars of type B5 and earlier are described by Henize et al. (1975). We report here preliminary results of a search for cool stars with anomalous excess brightness in the far ultraviolet. All stars with spectra observed to shortward of 2600Å have been catalogued, and although a detailed comparison with available stellar catalogs is still in progress, a few outstanding anomalies have already been detected and are discussed below. Flux data together with derived temperatures and absolute magnitudes for the companions will be reported later.

II. HOT COMPANION TO HR 3080

HR 3080 (= a Pup = HD 64440, V = 3.70) clearly shows a stronger ultraviolet continuum (figure 1, Plate ___) than is normal for a G5 III star. This spectral classification is by Woods (1955) at a resolution of about 1 Å. The star is known to be a single-line spectroscopic binary (Wright 1905; Christie 1936) with P=2660 days, but even in the near UV there is no photometric evidence of a hot companion. In fact, 13-color photometry (Mitchell et al. 1974), which includes magnitudes at 3370 and 3530Å, shows an energy distribution similar to that of the G8 III star μ Aur (Mitchell and Johnson 1969) and redder than that of most other G giants. Allowing for possible interstellar reddening, these data indicate that the secondary in HR 3080 is fainter than the G primary by at least 2 1/2 mag.

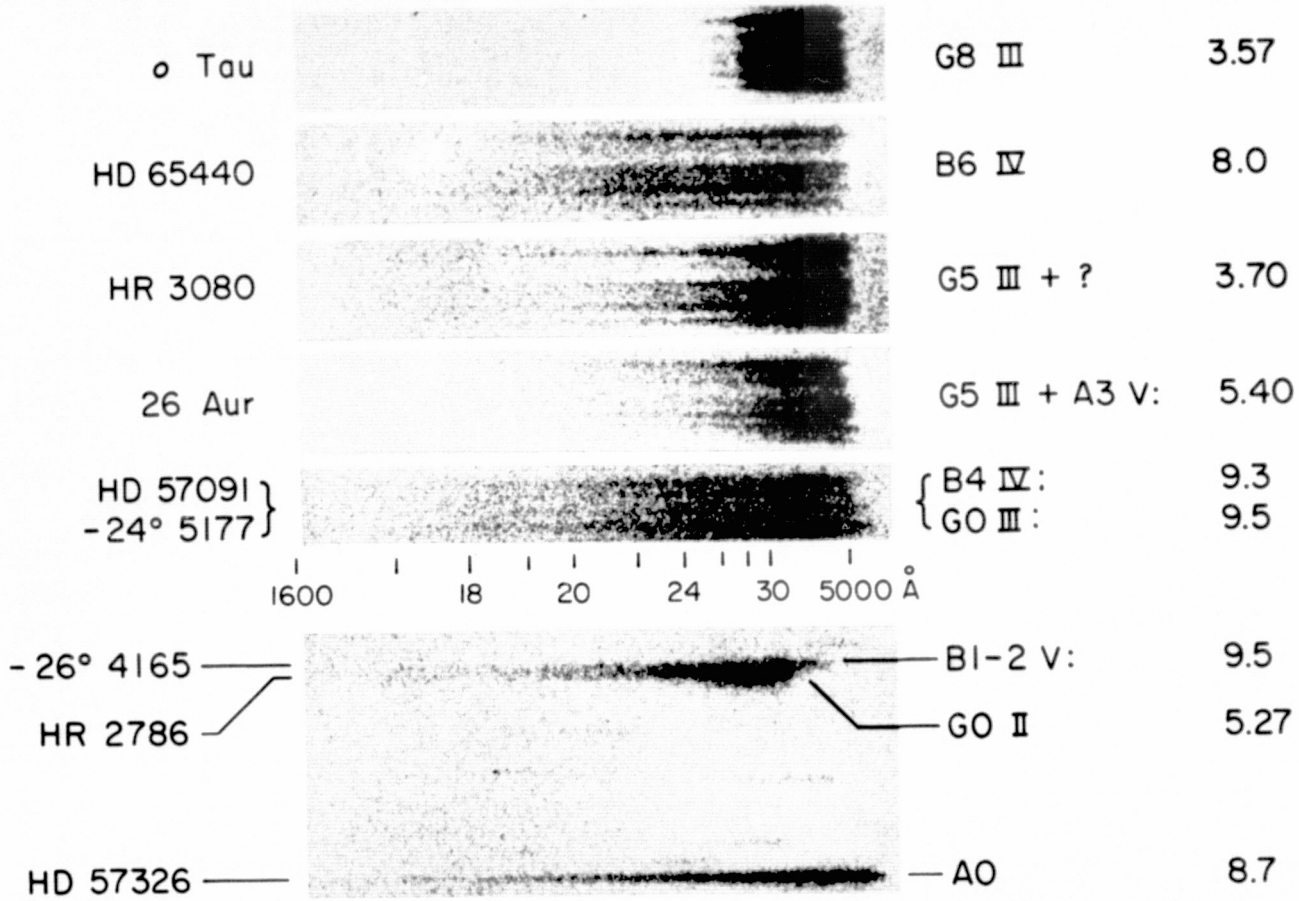

Figure 1. Ultraviolet Objective-Prism Spectra of some of the Stars Discussed and Comparison Stars. Visual magnitudes are given after the spectral types, which in some cases are newly derived. HR3080 shows radiation from a subluminous UV companion, probably B6 or earlier. HD 57091 overlaps a G-type star and has too flat a spectrum for its HD type of A0. Apparent excess flux from HR 2786 may be due to overlap from a B-type star; a nearby A0 star demonstrates the normal unwidened spectrum width and the characteristic slope for early A-type stars.

in U. A McDonald spectrogram (see section III), well-exposed in the near UV, shows perhaps a hint of contamination by a B-star spectrum. The Ca II K-line is weaker than usual, whereas Balmer lines appear slightly enhanced and other lines appear normal.

The Celescope photometry (Peytremann and Davis 1974) shows anomalous brightness in the U_3 band ($\lambda_{eff} \simeq 1600$Å), but this fact has not been commented upon. The U_3-V value is similar to that for HR 2786, shown in section III to have a hot star nearby. There are no other Durchmusterung stars near HR 3080 and the Palomar Sky Atlas southern extension (red print only) shows no stars in the vicinity which are likely to be contaminating the measurement.

Our Skylab observations of HR 3080, obtained on 30 December 1973, extend to about 1700Å and show, shortward of about 2600Å, fluxes similar to the stars HD 65440 (m_v = 8.0, type B8) and 65656 (m_v = 7.9, type B5) which are on the same exposure. A McDonald spectrogram of HD 65440 gives an MK type of B6 IV. The reddening of these stars is apparently small. The UV energy distribution of HR 3080 shows a definitely higher temperature than that of the A3 V companion ($m_v \simeq 6.4$) to 26 Aur. On the other hand, the UV spectrum is not dissimilar to an unwidened spectrum (not shown) of the extremely hot 10th mag. subdwarf CPD-31°1701 (Garrison and Hiltner 1973). This leads us to conclude that a definite temperature and visual magnitude should not be assigned to the hot companion of HR 3080 until a more accurate measurement of the flux distribution is made. However, for discussion purposes a preliminary estimate of spectral type $\leq$ B6 ($T_{eff} \geq 15000$K) will be assumed for the secondary,

giving U-V $\leq$ -0.6. Combined with the above constraint on the near UV brightness of the secondary and the measured U-V = 1.80 for HR 3080, this gives a difference in visual mag. $\Delta V \geq 4.9$, or $V_2 \geq 8.6$. The far UV flux appears to indicate $V_2 \leq 9$.

Both the parallax (0".023) and luminosity class give a visual absolute magnitude of about +0.5 for the G star. The ultraviolet companion thus has $M_V \sim +5.5$, which is approximately 6 mag. below the main sequence at class B6. This star is evidently a subdwarf lying somewhat above the normal white dwarf sequence.

Since the mass function of the system is known to be 0.35 $\mathcal{M}_\odot$ (Batten 1967) we may estimate the mass of the secondary by assuming a reasonable mass for the primary. According to Popper (1966), G giants range in mass from 2 to 4 $\mathcal{M}_\odot$ which leads to a lower limit for the secondary of 1.7 $\mathcal{M}_\odot$. This is greater than the Chandrasekhar limit and suggests that this star might be a Population I analog of the extended horizontal branch stars (Greenstein and Sargent 1974). However, the lower limit for the mass of the secondary is reduced to 1.4 $\mathcal{M}_\odot$ (within the Chandrasekhar limit) if the primary mass is reduced to 1.4 $\mathcal{M}_\odot$. In view of the uncertainties in the masses of G giant stars and in view of the further uncertainties introduced by the evolutionary effects discussed below it is possible that this star is a partially degenerate star on its way to the white dwarf sequence.

Following current theories of stellar evolution, it is reasonable to assume that the hot subluminous component has evolved through a

giant or supergiant phase. Since the orbital radius is 5 - 7 AU for any reasonable value (2 - 7$M_\odot$) of the combined mass of the system, mass transfer probably took place in this system when the present secondary reached its giant or supergiant stage. If the secondary became a supergiant, mass transfer must have been significant. The effect on the evolution and properties of the companion receiving the mass is, however, poorly understood at the moment (e.g., Kondo 1974).

The high eccentricity of this binary (e=0.4) suggests that the secondary may have experienced a supernova explosion. Although an eccentric orbit does not necessarily call for a supernova explosion, such an event almost inevitably turns an originally circular orbit into an eccentric one with a greater orbital radius (e.g., McCluskey and Kondo 1971). In this case, the explosion would probably strip away part of the envelope of the current primary and result in its current mass being less than normal.

The question of the masses of these stars may be resolved by radial velocity measures in ultraviolet spectra of the secondary and by observations of a possible eclipse effect on the secondary. We are proposing to perform such observations with the International Ultraviolet Explorer (IUE) satellite scheduled for launch in 1977. Radial velocity observations in the blue are also needed to update the spectroscopic orbit in order to refine the date of next periastron passage, estimated to be in late 1978.

III. CATALOG ERRORS AND DEFICIENCIES

Several apparent cases of anomalous G stars turned out to be

due to errors or deficiencies in the star catalogs. In some cases an early-type star, not contained in the SAO Star Catalog on which most of our identification work is based, is close enough to the G star to produce the observed spectrum. In other cases the listed SAO spectral type appears to be in error. A few instances are worth noting here.

When possible, where there is insufficient or nonexistent previous spectral information on the UV source, we are obtaining ground-based spectral classifications to aid our tie-in with visible-wavelength studies. The spectrograms, photographed by Wray with the 91 cm reflector at McDonald Observatory using the Meinel spectrograph with Bowen Schmidt camera and two-stage RCA image tube, are normally widened to 1.2 mm with a dispersion of 82Å/mm and resolution nearly the same as that of the Kitt Peak Atlas (Abt et al. 1968).

HD 57091 (= CoD -24° 5178, m_v = 9.3, type A0) is not in the SAO Star Catalog and was originally identified by us as the SAO star CoD -24° 5177 (m_v = 9.5, type G) less than 1' away. However, after proper identification some discrepancy still exists, the UV flux (figure 1, Plate ___) being considerably too bright for an A0 star of that magnitude. Slightly-widened (0.3 mm) McDonald spectrograms give spectral classes of about B4 IV and G0 III for HD 57091 and -24° 5177, respectively. Thus the HD class A0 is inaccurate and the UV energy distribution is now accounted for, although the flux level suggests that m_v is ~0.5 mag. brighter than given for HD 57091.

HD 204185 (=BD +60° 2234, m_v = 8.1) has an HD spectral type of G0 but is far too bright in the ultraviolet. We find from Bidelman's

spectral data file that Petrie and Pearce (1962) classified it as B3e. The HD class thus appears to be in error.

HD 36781 (= BD -01°948, m_v = 8.5) is erroneously listed by the SAO Star Catalog (star no. 132266) as having spectral type F2, whereas the HD type is B9 and the MK type is B6 V (Schild and Chaffee 1971).

HR 2786 (= HD 57146, V = 5.27), a G0 II star, was noted by Parsons and Peytremann (1973) to be abnormally bright in the Celescope U_3 band, but since no companion was known they suspected chromospheric emission as the cause. The unwidened exposure illustrated in figure 1 (Plate ___) shows that a strong UV continuum exists which may be due to HR 2786 and/or a faint star nearby. Further research shows that it is most likely due to the other star, CoD -26°4165 (= CPD -26°1974, m_v = 9.5, not in SAO or HD), separated by 2!2. There is nothing abnormal evident in a near-UV McDonald spectrogram of HR 2786, while a slightly-widened (0.25 mm) spectrum of -26°4165 shows it to be an early B dwarf, probably B1-2 V. Thus, although the ultraviolet observations do not rule out a hot, faint companion to the G0 II star, they are best explained by contamination from the nearby B star. IUE observations can settle this question.

IV. OBSERVED COOL GIANTS WITH KNOWN HOT SECONDARIES

We list in table 1 the known ζ Aur, VV Cep, and similar systems which were photographed from Skylab, along with the times of the exposures and an approximate measure of the extent of the spectrum. The spectral types are taken from the literature. These systems will be discussed in detail later, and we solicit recent observations and other relevant information.

TABLE 1

OBSERVED SYSTEMS WITH KNOWN HOT SECONDARIES

Name	HD	Spectrum	Obs. λ*	Time JD 2440000+
HD 4492	101379/80	G0 + A0	2200	1839.35
HR 6497	157978/79	G2 Ib + A0	2000	1916.10
χ Cir	130701/02	G3 IIv.+ B8:	2400	1910.46
26 Aur	37269	G5 III + A3 V:	1800	2031.16
HR 5667	135345/46	G5 Ia + B	(2400)	1907.55
ζ Per	18925/26	G8 III:+ A3:	1700	1925.11
HR 3386	72737/38	K0 III + A3	1800	2037.25
31 Cyg	192577/78	K2 II + B3 V	1600	1840.40, 1905.34
32 Cyg	192909/10	K5 I + B3 V	2000	1840.40, 1905.34
ι Aur	32068/69	K5 II + B6 V	1600	1937.22
5 Lac	213310/11	M0 Iab + B	2000	1910.46
δ Sco	148478/79	M1 Ib+B + B4 V	1300	1911.49
HR 8164	203338/39	M1 Ibep+B + B2 V	1700	1917.39
HR 2902	60414	M2 Iep + B2 V	(2000)U	2013.16
μ Cep	208816	M2ep I + B	2200	1917.59, 1930.53, 2037.21

*Shortest wavelength at which definite flux was recorded in 4 min. widened exposure, or 4 1/2 min. unwidened (U).

This work is supported at the University of Texas under NASA contracts NAS 9-13176 and NAS 8-13176. We thank Messrs. R. McMillan and D. West for assisting with the McDonald observations.

REFERENCES

Abt, H.A., Meinel, A. B., Morgan, W. W., and Tapscott, J. W. 1968, An Atlas of Low-Dispersion Grating Stellar Spectra (Kitt Peak Nat. Obs.).

Batten, A. H. 1967, Pub. Dom. Ap. Obs. (Victoria), 13, 119.

Christie, W. H. 1936, Ap. J., 83, 433.

Garrison, R. F., and Hiltner, W. A. 1973, Ap. J. (Letters), 179, L117.

Greenstein, J. L., and Sargent, A. I. 1974, Ap. J. Suppl., 28, 157.

Henize, K. G., Wray, J. D., Parsons, S. B., Benedict, G. F., Bruhweiler, F. C., Rybski, P. M., and O'Callaghan, F. G. 1975, Ap. J. (Letters), 199, L

Kondo, Y. 1974, Ap. and Space Sci., 27, 293.

McCluskey, G. E., and Kondo, Y. 1971, Ap. and Space Sci., 10, 464.

Mitchell, R. I., Forbes, F. F., and Johnson, H. L. 1974, unpublished report to NASA; paper in preparation.

Mitchell, R. I., and Johnson, H. L. 1969, Comm. LPL, 8, 1 (no. 132).

Parsons, S. B., and Peytremann, E. 1973, Ap. J., 180, 71.

Petrie, R. M., and Pearce, J. A. 1962, Pub. Dom. Ap. Obs. (Victoria), 12, 1.

Peytremann, E., and Davis, R. J. 1974, Ap. J. Suppl., 28, 211.

Popper, D. M. 1966, Trans. IAU, 12B, 485.

Schild, R. E., and Chaffee, F. 1971, Ap. J., 169, 529.

Woods, M. L. 1955, Mem. Commonwealth Obs. (Mt. Stromlo), no. 12.

Wright, W. H. 1905, Ap. J., 21, 371.

G. F. BENEDICT, S. B. PARSONS and J. D. WRAY: Department of Astronomy, University of Texas, Austin, TX 78712.

K. G. HENIZE: NASA/Johnson Space Center, Code TE, Houston, TX 77058.

Y. KONDO: NASA/Johnson Space Center, Code TN23, Houston, TX 77058.

Appendix F

SKYLAB ULTRAVIOLET STELLAR ASTRONOMY EXPERIMENT S-019

Submitted to Applied Optics November 17, 1975

Appendix F

SKYLAB ULTRAVIOLET STELLAR ASTRONOMY EXPERIMENT S-019

Fred G. O'Callaghan, Karl G. Henize, and James D. Wray

ABSTRACT

An objective-prism stellar spectrograph of 15-cm aperture was flown on all three Skylab missions. The wavelength region from 1300 to 5000Å was covered by a special optical system containing a combination of reflecting telescope optics, a CaF_2 objective prism and an achromatized field corrector lens system of CaF_2 and LiF. Observations of 188 star fields, each covering 4.0 x 5.0 degrees, were conducted at the Skylab antisolar airlock with the aid of an articulated mirror system (AMS) which allowed acquisition within a 30 degree by 360 degree band of the sky.

Fred G. O'Callaghan - Boller & Chivens Division of Perkin-Elmer Corp., 916 Meridian Ave., S. Pasadena, CA

Karl G. Henize - The University of Texas at Austin, Austin, TX, and Johnson Space Center, Houston, TX

James D. Wray - The University of Texas at Austin, Austin, TX

I. Introduction

Objective-prism and objective-grating spectrographs are ideal instruments for obtaining large numbers of moderate resolution stellar spectra which are useful for classification purposes and to search for peculiar stars. It is particularly desirable to obtain a large statistical sample of such spectra whenever a new wavelength interval is being explored. Therefore, when the UV region became accessible with the advent of orbiting spacecraft a number of such instruments were devised and employed to explore the characteristics of UV stellar spectra. This paper describes an objective-prism spectrograph which has been used to survey stellar spectra in the 1300 to 3000 Å wavelength region to a limiting V magnitude of about 6.5.

In 1965 a study was undertaken at Northwestern University to design a compact spectrograph which could operate through the scientific airlock then planned for the hatch of the Apollo command module. Practical limitations were set by the aperture of the airlock (8 x 8 inches) and the very limited volume available for the stowage of the instrument. The stowage location was the volume later to be used for one of the lunar rock boxes, it being expected that the spectrograph would be flown only during the early earth-orbiting phase of Apollo. These limitations led to a 15-cm aperture f/3 modified Ritchey-Chretien optical system employing a 4° objective prism of calcium fluoride (CaF_2) as the dispersing element. The manufacture of five units was begun in 1966 and completed in late 1967. Unfortunately, the Apollo fire in early 1967 resulted in the removal of the scientific airlock from the Command Module hatch and it was not possible to carry out the anticipated observing program in the early

phases of Apollo. Instead, the project was transferred to the Skylab program and was eventually operated on all three of the Skylab missions. Operation from Skylab required slight modifications to the spectrograph (mainly a quick change mechanism for film magazines) and the addition of an articulated mirror system (AMS) which would allow the spectrograph line of sight to be pointed over a large area of the sky since maneuvering Skylab for experiment pointing was not feasible.

II. Spectrograph Optical System

The basic optical components of the spectrograph comprise an objective prism and a camera. Auxiliary optical systems include a finding telescope and a focussing microscope.

The camera consists of an f/3 Ritchey-Chretien system with a two-element achromatized astigmatism corrector and field flattener. Dimensions are listed in table 1. Both the primary and secondary mirrors are of fused quartz. The surfaces are hyperboloidal and are coated with aluminum overcoated with magnesium fluoride optimized to provide maximum reflectivity in the 1300 to 2000Å region.

The front corrector element is CaF_2 and the rear element is lithium fluoride (LiF). The front corrector surface is a free aspheric, the two inner air-spaced surfaces are spherical and rear surface is flat. Longitudinal chromatic aberration in these elements is negligible from 1400 to 3000Å but significant lateral chromatic aberration is present. At a distance of 10 mm off axis the 1600A and 1400A images are displaced 73 and 185 μm toward the plate center relative to the 2000A image. When operated without the prism the system produces low dispersion spectra for which the orientation and dispersion vary with field position. Such a mode was occasionally used during the Skylab observations to obtain information on very faint objects. The image quality obtained by the basic design is illustrated in figure 1.

Table 1

Dimensions and Performance Data For The S-019 Spectrograph

Objective prism aperture	15.88 cm
Primary mirror aperture	15.24 cm
Secondary mirror aperture	7.62 cm
System EFL	45.72 cm
Plate scale	451 arcsec/mm
Field size	4.0 x 5.0 deg
Image diameter (maximum)	33 μm @1600A (= 15 arcsec)
Wavelength resolution (corresponding to 33 μm)	2A @ 1400A, 12A @ 2000A, 42A @ 2800A

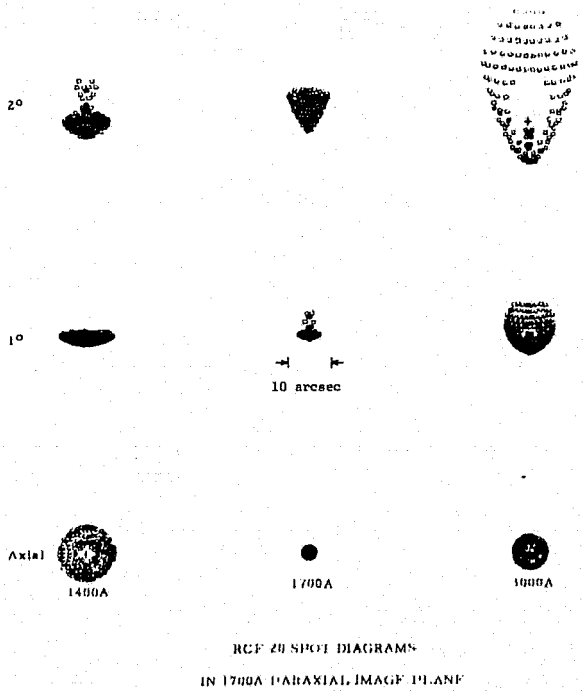

Figure 1. Ray Tracing Diagrams Showing the Theoretical Image Quality at Several Wavelengths and Several Field Angles.

The 4° objective prism is fabricated of CaF_2. The procurement of suitable material for these prisms was one of the greater challenges of this project. A facility was established at Northwestern University to measure the UV transmission of the CaF_2 prior to its acceptance and a cooperative effort was undertaken with Harshaw Chemical, the supplier, to test their entire stock of 8-inch boules. Only one was found to provide the uniformly high transmission desired but this was not sufficient to supply all the elements required. A year's experimentation and the construction of a new, larger furnace by Harshaw was required before a second satisfactory boule was obtained.

Problems with mounting the objective prisms were also encountered since CaF_2 is an easily deformed material. The initial method of mounting using special silicon rubber gaskets was not successful since the gaskets introduced sufficient strain to warp the elements. The solution to this problem was found by potting the prisms in their aluminum cells with an RTV compound.

Another technological challenge was the figuring of a free aspheric on the front surface of the CaF_2 corrector element. This task was undertaken by the optician, Frank Cooke, who, after considerable experimentation, evolved a fabrication method which produced corrector elements of high quality.

A finding telescope of 2.54-cm aperture, 7X magnification and 7° field was provided for visual confirmation of telescope pointing by the astronaut. A pressure seal window was provided at the rear of the optical canister. The lamps illuminating the reticle are powered by a rechargeable nickel-cadmium battery so no electrical interface to spacecraft power was needed.

A 30X focus microscope was incorporated into the film magazine to allow for visual verification and adjustment of camera focus. This system was useful in initial laboratory optical testing and it was also anticipated that it could be used for refocussing the camera in orbit. However, the mechanical and thermal stability of the camera was such that such refocussing was never required.

Howard Padgett of Cook Electric Co. was the optical engineer responsible for the design of these optical systems and their translation into an operating instrument.

III. Spectrograph Mechanical Components

The spectrograph consists of two major components - an optical canister and a film canister. The optical canister houses the prism and camera optics as well as the objective section of the finding telescope. The film canister houses the film slides, the shutter and film transport system, the eyepiece of the finder and the focussing microscope. The general configuration of the spectrograph is illustrated in Figure 2.

Both canisters were fabricated from aluminum castings. Since these canisters became a part of the spacecraft pressure hull when the airlock door was opened, their structural integrity was subject to stringent specifications. It was required that the casting meet class 1 x-ray specifications as well as dye penetrant and vacuum leak tests. However, meeting the x-ray specifications was found to be impossible and finally class 2 castings were accepted and a hydrostatic pressure test to 100 psi was accepted by NASA as sufficient proof of structural integrity. The canisters were sealed to each other and the optical canister was sealed to the AMS by vacuum flanges incorporating double row Viton "O" rings and special Gask-O-Seals designed for the purpose. Vacuum tight covers were provided so that both canisters could be evacuated for stowage.

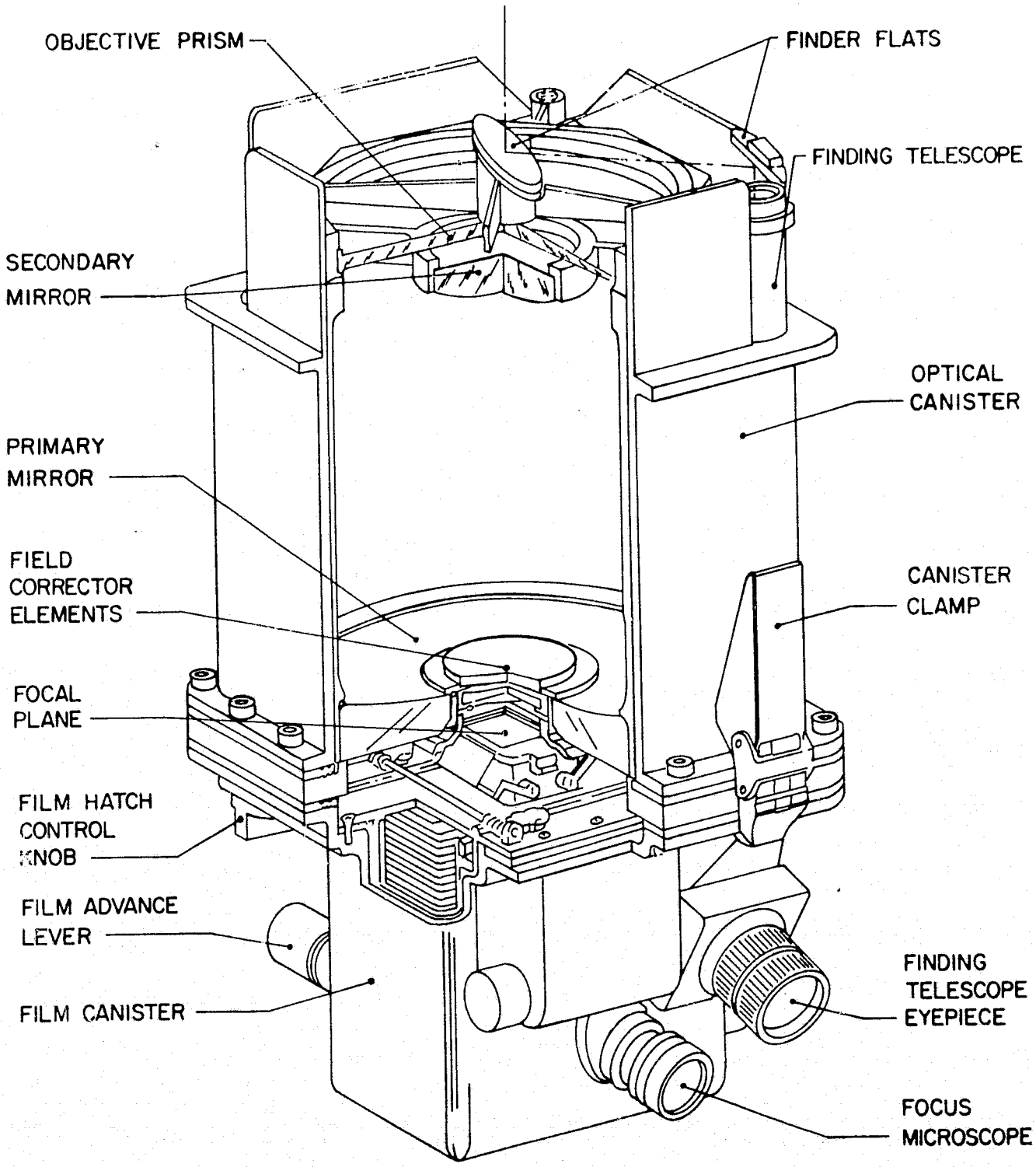

Figure 2. Diagram showing the Optical and Mechanical Components of the Objective-Prism Spectrograph.

These assemblies were tested with a helium leak detector to a specification of 1×10^{-6} standard cc/sec (0^2).

The prism and mirrors were mounted in the optical canister with invar cells and spacers which effectively eliminated any thermal effects on focus. The prism cell was removable in orbit so the instrument could be operated with or without the prism as desired.

The film transport system consists of a lever-operated mechanism which positions successive film slides on the optical axis, moves them into the focal plane, then opens and closes the shutter. The film was mounted on perforated stainless steel platens by means of snap-over nylon covers. These platens were then mounted in the film canister in two stacks with the stainless steel of each platen bearing directly on the nylon cover of the slide below. Each canister held approximately 162 slides, but since the reliability of the transport system was found to depend critically on the compression forces within the stacks, this number varied by ±2 from canister to canister.

A complicating factor in the optical design was the fact that it was impossible to place the focal plane so that it cleared the back surface of the primary mirror. Thus it was necessary to design a "carriage" which would first receive a fresh film slide, then transport it forward to the focal plane. Positive focal plane registration was accomplished by butting the film carriage against a definitive stop ring in the optical canister. Focus adjustment was accomplished by mounting the stop ring on a precision screw mechanism which could be driven by an external knob.

The design and construction of the spectrograph mechanical components was carried out by Cook Electric Co. of Morton Grove, Ill.

IV. The Articulated Mirror System

When the S-019 spectrograph was assigned to the Skylab mission it was necessary to design a means for pointing the line of sight over a large area of the sky. A mirror system for this purpose was designed by F. G. O'Callaghan and Norman Page, and a prototype unit was constructed at Northwestern University. Final design and construction of flight units was carried out by the Boller & Chivens Division of Perkin-Elmer Corp. This system consists of a large flat mirror, gear systems for extending it through the airlock and then tilting and rotating it, and a spectrum-widening mechanism. Its general configuration is illustrated in figure 3.

The mirror is fabricated from CER-VIT. It is elliptical with major and minor axes of 38 and 19 cm respectively. It has a ribbed structure supporting a face plate 1 cm thick. The surface was finished to 1/8 wave accuracy at 6300A and its coating is similar to that of the camera mirrors.

Extension of the AMS mirror out of the canister, past the airlock door, into space is accomplished via a manually operated extension mechanism. The mechanism is a double telescoping device which is guided and extended by four ball screw nut combinations. The use of ball screws in this way reduced friction to a very low value and made reliable manual operation possible. The AMS mirror was mounted on a fork which in turn was mounted on a pair of very thin ball bearings. Rotation of the fork on the bearings through a range of 360° allowed for the rotation movement of the mirror. Tilt was accomplished by rotation of the mirror about the fork tines via a tangent arm mechanism. A total adjustment range of 15° of mirror tilt (30° of change in the line of sight) was available. Tilt and rotation adjustments were made through a single dynamic member by means of two pinion gears and a differential gear train.

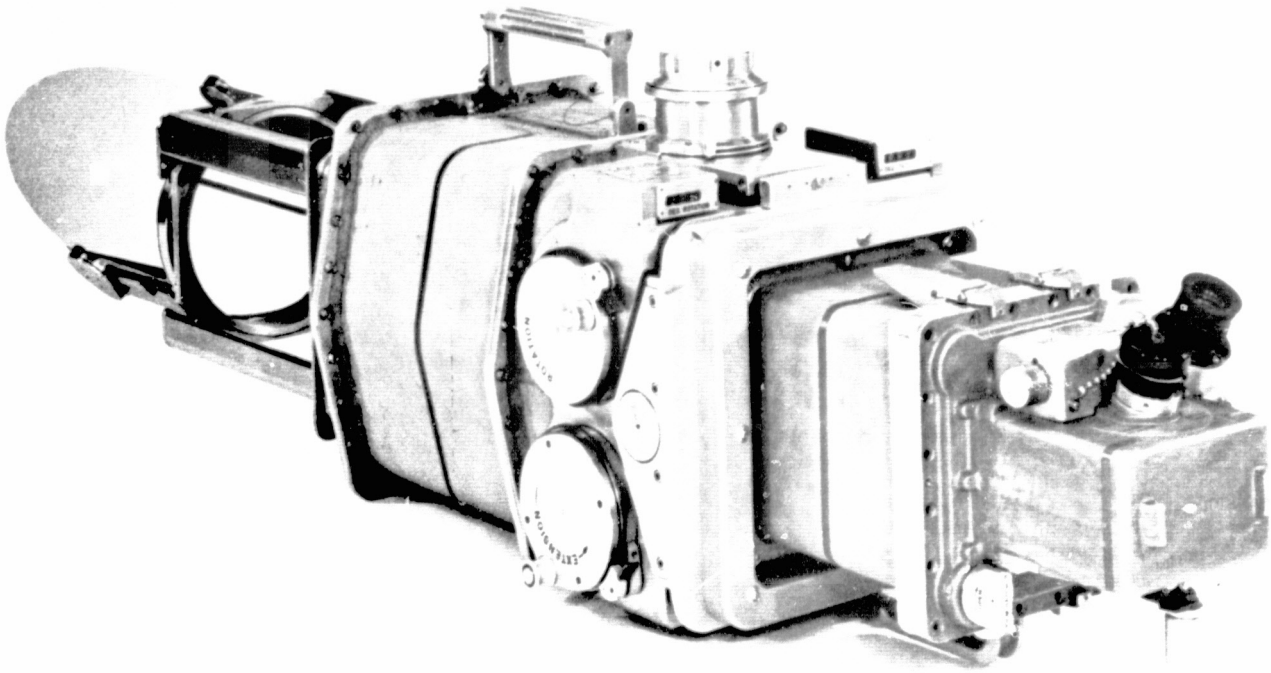

Figure 3. Photograph of the Articulated Mirror System with the Spectrograph Attached. The mirror is shown in its extended position. The cylinder on the top of the mirror canister is the control and drive mechanism for spectral widening.

When the pinions were driven through the same angle, rotation of the mirror resulted. Differential motion of the pinion gears resulted in tilt of the mirror. Torque was transmitted via splines, gears and manual crank handles. Gear driven counters, reading to 0.1°, were provided to enable the astronaut to point the AMS mirror to the desired star field by means of pointing angles calculated on the ground.

Spectral widening was accomplished by rotation of the rear nest assembly which carried the spectrograph. A total widening of 270 arcsec was obtained by a spring motor drive which could be operated at any of three rates; 30, 90, and 270 sec for full 270 arcsec widening. Vacuum seals between the static canister and the rear nest airlock assembly were double "O" ring seals sliding on a flat surface.

The rear nest airlock assembly is a manually actuated 8-point pivot roller assembly that locks and seals the experiment flange in place. Compression of a double line Gask-O-Seal gives metal-to-metal contact thus providing electrical bonding across the interface. This is similar in design tothe original scientific airlock clamping mechanism except for certain improvements including use of roller bearings to reduce friction. These improvements were later incorporated by NASA into the airlock design.

To ensure that the failure of one instrument would not block the use of other instruments in the airlock, NASA required the incorporation of a jettison system which could eject all mechanisms which extended beyond the airlock door line. A CO_2 gas-powered system was developed which met this requirement. The system was activated by CO_2 gas pressure which first detached the main mirror carriage by delatching the heads from specially designed two-piece bolts and the pressurized four pistons located within the ball screw shafts to impart a ≈ 2 meter/sec velocity to the mirror assembly.

C.2

In contrast to the cast construction of the spectrograph canisters, the AMS canister sections were machined from solid billets. The latter method proved to be a more effective way to obtain canisters with the required structural integrity. All rotary penetrations through the canister walls were sealed with triple Viton "O" ring seals. This technology provided a simple means of meeting the NASA structural integrity and vacuum leak requirements and no difficulties were encountered in meeting such requirements.

The AMS proved to be a useful general purpose facility which allowed several other experiments (S-063, S-073, S-183, and S-201)[1] to also achieve some flexibility of pointing through the anti-solar scientific airlock.

V. Photographic Film

The UV sensitive, Schumann-type Kodak 101-06 Estar-base film was used in this program. The method of supporting this pressure-sensitive film on steel platens is described in Section III.

A special problem with this emulsion is its tendency to fog when in close proximity to bare metal. Although such sensitivity to aluminum is known it was believed that stainless steel produced no such results. However we encountered a weak fog on nearly all frames which showed a hole pattern corresponding to that of the stainless steel platens. Since this fog does not appear on the regions of the emulsion protected by the nylon covers we conclude that cause of the fog is associated with long exposure to stainless steel in vacuum conditions. An average fog density of approximately 0.6 was reached during the 100-day exposure (from canister loading to unloading) of Skylab 4. The areas protected by the nylon show a lighter fog that reached a density of 0.39 during the Skylab 4 mission. This lighter fog is assumed to be a combination of thermal and radiation fog. The estimated radiation dose that contributed

to this effect was 1.91 rad.

A calibration facility was established at Northwestern University and later moved to the University of Texas where all flight film received both pre-flight and post-flight calibration. This system consisted of an H_2 microwave discharge lamp, a 3/4 meter monochromator, a beam sample photometer with filter assembly, a Mg F_2 field lens assembly, and a 6-inch f/15 Cassegrain collimator, all mounted in a high performance vacuum system. A bellows assembly was used to mount the spectrograph. This system , with appropriate modifications, was also used to produce and test the high-reflectivity UV coatings used in the experiment.

VI. Experiment Results

This experiment was operated on all three Skylab missions and a total of 188 star fields were observed in the prism-on mode. It was found that widened 270 second exposures produced measurable fluxes at 1500A of unreddened B0 stars as faint as V = 7.0. A total of 1600 stars show measurable fluxes at 2000A and 400 show measurable fluxes at 1500A. Of these, about 170 show evident absorption or emission lines. Spectra in a representative field are illustrated in figure 4.

These spectra are being analyzed at the University of Texas in Austin by means of a PDS 1010A microdensitometer controlled by a PDP-8/e computer. Preliminary scientific results include a study of the intensities of the strong C IV and Si IV lines over a wide variety of spectral types and luminosities,[2] studies of 12 Wolf-Rayet stars which show emission lines shortward of 2000A,[3] detection of a previously unknown blue subdwarf companion to a G star[4] and the identification of several unusual emission lines in the spectrum of β Lyrae.[5]

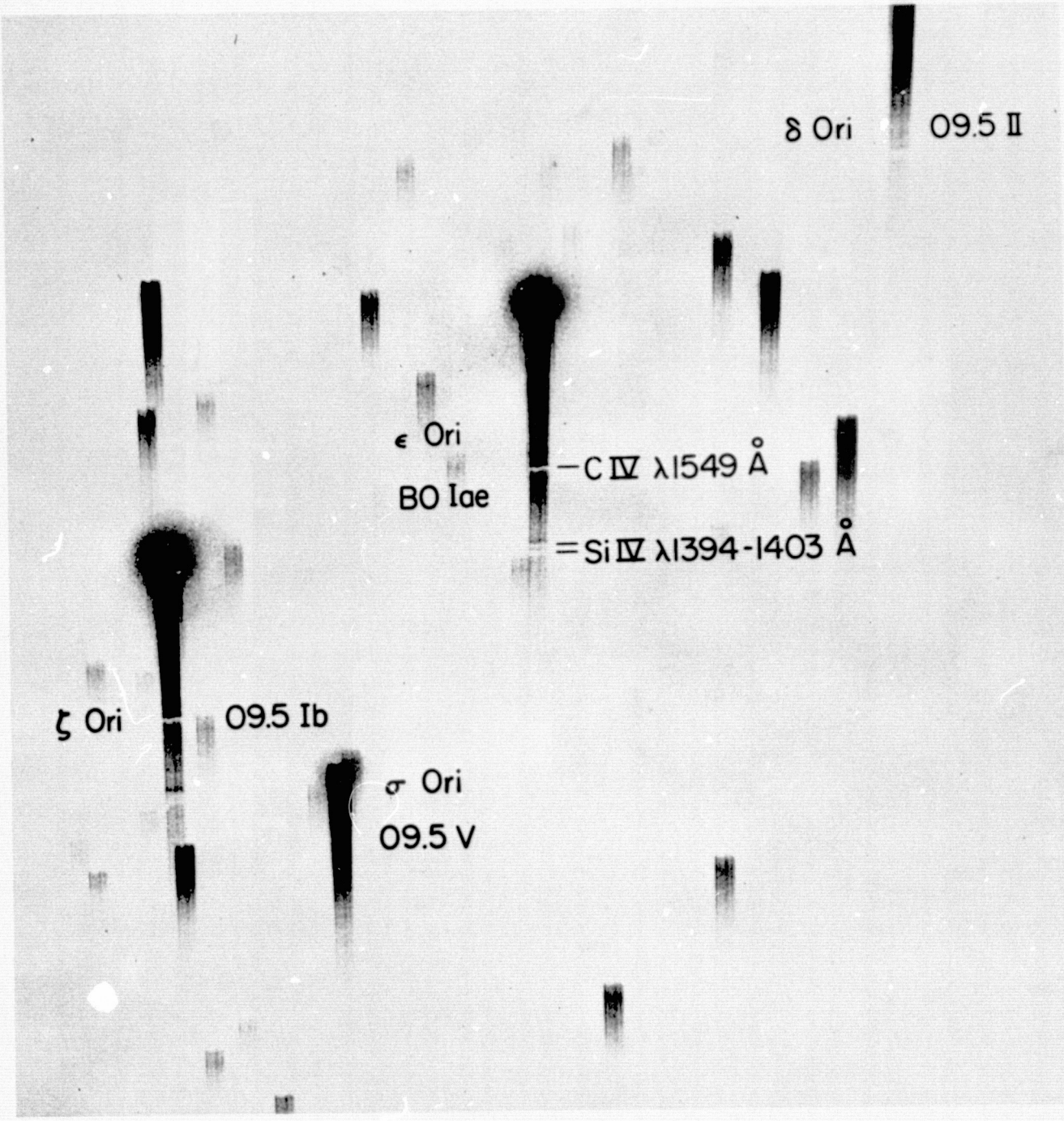

Figure 4. Representative Spectra taken with the S-019 Spectrograph. The supergiant stars ζ and ε Ori show conspicuous absorption lines flanked by redward emission at Si IV λλ 1394, 1403 and C IV λ1549. Note that the main sequence star σ Ori shows only weak absorption at C IV λ1549.

Acknowledgements

The concept for this experiment originated at Northwestern University, Evanston, Illinois. That institution was responsible for the construction of the spectrograph and the AMS under NASA contract NAS 9-7222. Planning of the Skylab observations and the analysis of the data have been carried out at the University of Texas at Austin. We wish to acknowledge the important contributions of Norman Page and Lloyd Wackerling at Northwestern University and of Sidney Parsons, George Benedict and Paul Rybski in the work at the University of Texas. Special thanks are also due to the many NASA engineers and contract officers who have given technical and administrative support to this program in innumerable ways. The work at the University of Texas has been carried out under NASA contracts NAS 9-13176 and 8-31459.

References

1. Applied Optics (In Press)

2. K. G. Henize, J. D. Wray, S. B. Parsons, G. F. Benedict, F. C. Bruhweiler, P. M. Rybski and F. G. O'Callaghan, Astrophysical Journal Letters 199, L119 (1975).

3. K. G. Henize, J. D. Wray, S. B. Parsons and G. F. Benedict, Astrophysical Journal Letters 199, L173 (1975).

4. S. B. Parsons, J. D. Wray, Y. Kondo, K. G. Henize, and G. F. Benedict, Astrophysical Journal 203, in press (1976).

5. Y. Kondo, S. B. Parsons, K. G. Henize, J. D. Wray, G. F. Benedict and G. E. McCluskey, Astrophysical Journal, in press (1976).